DSSR: an integrated software tool for Dissecting the Spatial Structure of RNA

User Manual for DSSR 2.3.2 (the Basic Version)

for noncommercial use only

Last updated: September 15, 2021

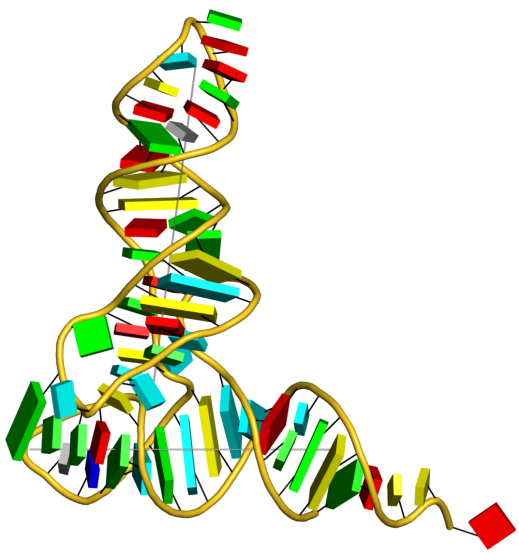

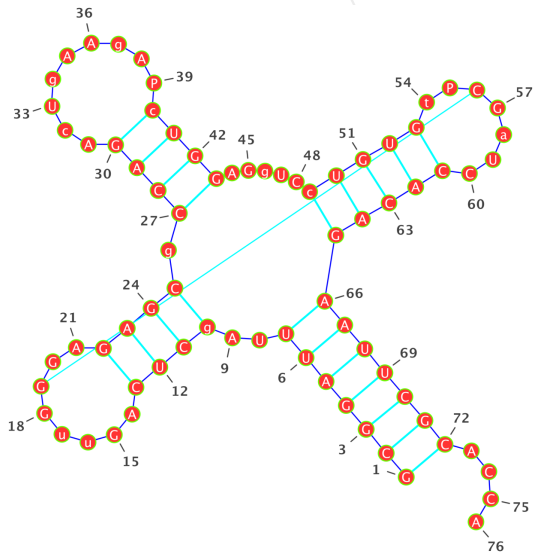

modified nucleotide, non-canonical base pair, helix, stem, coaxial stacking
hairpin/internal/junction loop, kink turn, G-quadraplex, i-motif, pseudoknot
cartoon-block innovative schematics in PyMOL, SQL-like feature queries in Jmol
in silico base mutations, regular helical models, customized rebuilding

by **Dr. Xiang-Jun Lu (律祥俊)**

Department of Biological Sciences
Columbia University, New York

- DSSR is licensed by Columbia University.

- DSSR is distributed in two variants:
  1. DSSR Basic covers features described in the three DSSR papers[1–3] to ensure that reported results can be *fully* reproduced. It is free for academic use.
  2. DSSR Pro includes advanced capabilities for model building, additional features in structural analyses, annotations, and visualizations. It is for paid users only.

- This user manual documents DSSR Basic. It is free and open to the public.

- The DSSR Pro manual documents the full-featured DSSR. It is available to paid users only.

- A brief summary and background information of DSSR can be found in the overview PDF.

Contents

1 Introduction **4**

2 Download and installation **8**

3 Analysis and annotation **8**

3.1 Command-line help . . . 8

3.2 Default run on PDB entry 1msy: detailed explanations . . . 10

3.2.1 Summary section . . . 11

3.2.2 Base pairs . . . 13

3.2.3 Multiplets (higher-order coplanar base associations) . . . 19

3.2.4 Helices . . . 22

3.2.5 Stems (canonical pairs with continuous backbones) . . . 23

3.2.6 Isolated canonical pairs . . . 23

3.2.7 Base stacks . . . 24

3.2.8 Atom-base capping interactions . . . 24

3.2.9 Various loops . . . 25

3.2.10 Single-stranded fragments . . . 26

3.2.11 2D structure in dot-bracket notation . . . 26

3.2.12 Structural features per nucleotide . . . 28

3.2.13 Backbone torsion angles and suite names . . . 29

Main chain conformational parameters . . . 29

Virtual torsion angles . . . 30

Sugar conformational parameters . . . 31

Assignment of sugar-phosphate backbone suite names . . . 32

3.3 Default run on PDB entry 1ehz ($tRNA^{Phe}$): summary notes . . . 33

3.3.1 Brief summary . . . 33

3.3.2 Modified nucleotides . . . 34

3.3.3 The four triplets . . . 34

3.3.4 Relationship between helices and stems . . . 34

3.3.5 Three hairpin loops . . . 35

3.3.6 One four-way junction loop . . . 35

3.3.7 Pseudoknot . . . 36

3.4 Default run on PDB entry 1jj2: four auto-checked motifs 36
3.4.1 Kissing loops 38
3.4.2 A-minor motifs 38
3.4.3 Ribose zippers 41
3.4.4 Kink turns 41
3.5 Identification and characterization of G-quadruplexes 43
3.6 Pseudoknots detection and removal 44
3.6.1 Higher-order pseudoknots 46
3.6.2 Pseudoknot removal 46
3.7 The `--more` option 47
3.7.1 Extra characterization of base pairs 47
3.7.2 Orientation of helices/stems 48
3.7.3 Base-pair morphology parameters for helices/stems 49
3.8 The `--non-pair` option 50
3.9 The `--json` option 52
3.10 The `--pair-only` option 53
3.11 The `--nmr` option 53
3.12 The `--get-hbond` option 54
3.13 The `--idstr` option 56
3.14 The `--symmetry` option 57
3.15 The `--prefix` option 57

4 Visualization features **57**
4.1 DSSR-Jmol integration 58
4.2 DSSR-PyMOL integration 58

5 Modeling capabilities **58**

6 Frequently asked questions **60**
6.1 What does DSSR stand for? 60
6.2 How does DSSR compare with other tools? 60
6.3 How is DSSR related to 3DNA? 60
6.4 What are the differences between DSSR Basic and DSSR Pro? 61

7 Acknowledgements **61**

References 61

List of Figures

1 Definitions of key nucleic acid structural components in DSSR 5
2 Three- and two-dimensional structure images of PDB entry 1msy 12
3 Parallel M+N and antiparallel M–N orientations between two nucleobases . . 15
4 Lenotis-Westhof definition of three edges and the *cis*/*trans* orientations . . . 16
5 Issues with the three edges in the Leontis-Westhof definition 17
6 Six types of G·A pairs involving the minor-groove edge of G 19
7 Pictorial definitions of rigid-body base morphology parameters 20
8 Base triplet (`GUA`) identified in PDB entry 1msy 21
9 Common secondary structural elements of RNA 25
10 Base pentaplet (`AUAAG`) identified in PDB entry 1jj2 37
11 Kissing-loop motif identified in PDB entry 1jj2 39
12 Types I and II A-minor motifs identified in PDB entry 1jj2 40
13 Ribose zipper identified in PDB entry 1jj2 42
14 Normal k-turn identified in PDB entry 1jj2 43
15 Schematic representation of G-quadruplexes 44
16 Topological descriptors and V-shaped loops of G-quadruplexes 45
17 Additional parameters calculated with the `--more` option 48
18 DSSR-Jmol featured in the cover image of NAR 59

1 Introduction

As the number of experimentally solved RNA-containing structures grows, it is becoming increasingly important to characterize the geometric features of the molecules consistently and efficiently. Existing RNA bioinformatics tools are fragmented, and suffer in either scope or usability. DSSR[1] is an integrated software tool for **D**issecting the **S**patial **S**tructure of **R**NA, designed from ground up to streamline the analyses/annotation of 3D RNA structures. Figure 1 outlines some key algorithms underlying the DSSR program.

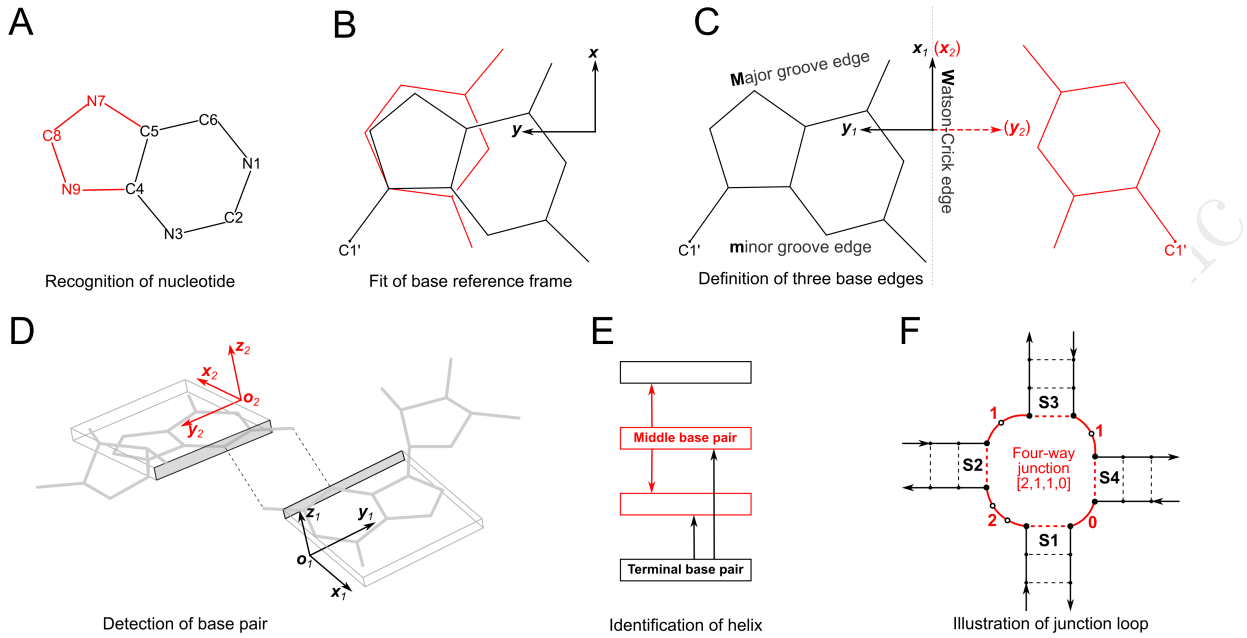

Figure 1: Definitions of key nucleic acid structural components in DSSR (Reproduced from Figure 1 of the DSSR paper[1]). (A) Nucleotides are recognized using standard atom names and base planarity. This method works for both the standard bases (A, C, G, T and U), and those of modified nucleotides, regardless of their tautomeric or protonation states. (B) Bases are assigned a standard reference frame[4] that is independent of sequence identity: purines and pyrimidines are symmetrically placed with respect to the sugar. (C) The standard base frame is derived from an idealized Watson-Crick base pair, and defines three base edges (Watson-Crick, minor groove, and Major groove) that are used to classify pairing interactions. (D) Base pairs are identified from the coplanarity of base rings and the occurrence of hydrogen bonds. This geometric algorithm can find canonical (Watson-Crick and G–U wobble) as well as non-canonical pairs. Higher-order (three or more) coplanar base associations, termed multiplets, are also detected. (E) Helices are defined by stacking interactions of base pairs, regardless of pairing type (canonical or otherwise) or backbone connectivity (covalently connected or broken). A helix consists of at least two base pairs. The same algorithm is applied to identify continuous base stacks that are outside of helical regions, by using bases instead of pairs as the assembly unit. Nucleotides not involved in base-stacking interactions are collected into one separate group. A stem is defined as a special type of helix, made up of canonical pairs and with a continuous backbone along each strand. Coaxial stacking is defined by the presence of two or more stems within one helix. An isolated canonical pair is one that is not contained within a stem. (F) 'Closed' loops of various types (hairpin, bulge, internal, and junction loops) are delineated by stems or isolated pairs, and specified by the lengths of the intervening, consecutive nucleotide segments.

Starting from an RNA structure in Protein Data Bank (PDB) or PDBx/mmCIF format, DSSR uses standard atom names and base planarity to detect nucleotides, including modified ones (Figure 1A). It employs the standard base reference frame (Figure 1B, C)[4] and a set of simple geometric criteria (Figure 1D) to identify all existent base pairs (bp): either canonical Watson-Crick (WC) and wobble pairs, or non-canonical pairs with at least one hydrogen bond (H-bond). The latter pairs may include normal or modified bases, regardless of tautomeric or protonation state. DSSR uses the six standard rigid-body bp parameters (shear, stretch, stagger, propeller, buckle, and opening) to rigorously quantify the spatial disposition of any two interacting bases. Where applicable, the program also denotes a bp by common names (e.g., WC, reverse WC, Hoogsteen A+U, reverse Hoogsteen A–U, wobble G–U, sheared G–A, imino G–A, Calcutta U–U, dinucleotide platform), the Saenger classification scheme[5] of 28 H-bonding types, and the Leontis-Westhof nomenclature[6] of 12 basic geometric classes.

DSSR detects multiplets (triplets or higher-order base associations) by searching horizontally in the plane of the associated bp for further H-bonding interactions. The program determines double-helical regions (Figure 1E) by exploring vertically in the neighborhood of selected bps for base-stacking interactions, regardless of backbone connection (e.g., coaxial stacking of helices). DSSR then identifies hairpin loops, bulges, internal loops, and multibranch (junction) loops (Figure 1F). The program outputs RNA secondary structure in three commonly used formats—dot-bracket notation (dbn), connectivity table (`.ct`), and bp sequence (`.bpseq`)—that can be fed directly into visualization tools such as VARNA[7]. DSSR derives proper dbn for RNA with higher-order pseudoknots, and it can also produce pseudoknot-free secondary structures.

In DSSR, each helix/stem is characterized by a least-squares fitted helical axis, and dinucleotide steps are classified into the most common A-, B- or Z-form double helices (where appropriate) and quantified by helical parameters. DSSR calculates commonly used backbone torsion angles (including the virtual η/θ torsions), classifies the backbone into BI/BII conformations and the sugar into C2′/C3′-endo-like puckers, and assigns the consensus RNA backbone suite names[8]. The program also identifies A-minor interactions, splayed-apart dinucleotide conformations, atom-base capping interactions, ribose zippers, G quadruplexes, i-motifs, kissing loops, U-turns, and k-turns, etc. Furthermore, DSSR reports non-pairing interactions (H-bonding or base-stacking) between two nucleotides, and contacts involving phosphate groups.

DSSR has been integrated to Jmol, a widely used Java/JavaScript viewer for 3D structures. The DSSR-Jmol integration[2] bridges the DSSR command-line analyzing tool and the Jmol

molecular viewer together via a simple JSON interface and a powerful query language. Users can now select DSSR-derived RNA structural features (such as base pairs, double helices, and various loops) as easily as they can select protein α-helices and β-strands. Moreover, fine-grained characteristics of these features can be queried via Jmol SQL for DSSR (see the DSSR-Jmol manual). Notably, the novel representation styles (step diagram and base blocks) and coloring schemes bring RNA visualization to an entirely new level (see Figure 3 of the DSSR-Jmol paper).

DSSR supersedes the 3DNA suite of programs[9–11] for the analysis, rebuilding, and visualization of 3D nucleic acid structures. It has been created from scratch by employing my extensive experience in supporting 3DNA, increased knowledge of RNA structures, and improved C programming skills. The software has a set of unique features not available elsewhere (to the best of my knowledge). By connecting dots in RNA structural bioinformatics, it makes many common tasks simple and advanced applications feasible. DSSR is efficient and robust, with sensible default settings and an intuitive output; thus it is accessible to a much broader audience than the classic 3DNA distribution (up to v2.4).

There is actually more to DSSR than meets the eye. DSSR Basic does not contain modeling features, or advanced variations of documented options herein. Please support DSSR by obtaining a paid license from Columbia University for DSSR Pro and the corresponding User Manual.

DSSR is being actively maintained and developed. As always, I greatly appreciate user feedback. So far, all reported bugs have always been promptly responded and fixed where appropriate. The program has been checked using all nucleic acid-containing entries in the PDB, without any known issues. Simply put, I strive to make DSSR a practical tool that the user community can count on.

When reporting bugs or submitting feature requests, please provide the specific DSSR version you are using (with `-v` or `--version`). For example, the version that the manual is based upon corresponds to (`x3dna-dssr -v`):

```
              DSSR: an Integrated Software Tool for
             Dissecting the Spatial Structure of RNA
              v2.3.2-2021jun29 by xiangjun@x3dna.org

As of version 2, DSSR may be LICENSED from Columbia University.
DSSR basic is FREE for academic uses, with ABSOLUTELY NO WARRANTY.
DSSR Pro is available for paid academic or commercial users only,
and it is actively maintained and continuously improved.

This is DSSR *basic*. Advanced features are available in DSSR Pro.
```

2 Download and installation

As of version 2.0, DSSR has been licensed by Columbia University for all uses. Please visit the Columbia Technology Ventures (CTV) website on DSSR for details.

The CTV distributes DSSR Basic and Pro versions in zip format for macOS, Linux, and Windows. Each zip file contains a DSSR binary executable as well as the associated user manual. The DSSR executable (`x3dna-dssr` for macOS and Linux, and `x3dna-dssr.exe` for Windows) is self-contained and does not rely on any third-party libraries. There is no need for any setup or configurations: type `x3dna-dssr -h` to verify your installation. Note that DSSR is a command-line program: you need a terminal window to run it.

DSSR Basic remains free for academic uses, and it comes with ABSOLUTELY NO WARRANTY. For long-term stability of the project, DSSR Pro and its corresponding User Manual (in PDF) are available for *paid users* only. The DSSR Pro manual documents (new and enhanced) features not available elsewhere.

DSSR is stable in terms of fundamental functionality and main output format. Where possible, I will try to maintain backward compatibility in future releases. If you only need fundamental features, you may not need to bother with frequent updates. DSSR is designed with simplicity and robustness in mind: get the job done, and then stay out of the way. On the other hand, DSSR is being actively maintained and developed, with new features added and known bugs fixed. Users are advised to keep up to date: it is as simple as downloading DSSR again from the CTV website to replace (i.e., overwrite) the old copy.

3 Analysis and annotation

Although the above introduction summarizes DSSR's major functionality in dry, 'abstract' technical terms, using DSSR effectively is very straightforward. This is best illustrated with concrete examples.

3.1 Command-line help

As is the norm of Linux/Unix command-line tools, running DSSR with `-h` (or `--help`) provides help information, as shown below (`x3dna-dssr -h`):

```
Usage: x3dna-dssr [options]
```

```
Each option is specified via --key[=val] (or -key[=val] or key[=val];
i.e., two/one/zero preceding dashes are all accepted), where 'key' can
be in either lower, UPPER or MiXed case. Options can be in any order.
Options:
  --help          Print this command-line help information (-h)
  --version       Print version number and exit (-v)
  --citation      Print preferred citation(s) and exit
  --input=file    Specify a PDB/mmCIF file for analysis (-i=file)
  --output=file   Designate the main DSSR output file (-o=file)
  --more          Report detailed bp and step/helical parameters
  --non-pair      Check non-pairing H-bonds/stacking interactions
  --pair-only     Output just base-pairing information [10x faster]
  --json          Generate output in JSON format for easy parsing
  --nmr           Process an ensemble of NMR structures
  --blocview      Generate cartoon/blocks, in extended view, in PyMOL
  --frame         Reorient a structure with specified base/pair frame
  --get-hbond     Report a list of H-bonds within nucleic acids

Examples:
  x3dna-dssr -i=1msy.pdb
  x3dna-dssr -i=1msy.cif --more --non-pair
  x3dna-dssr -i=1ehz.pdb -o=1ehz.out  # yeast phenylalanine tRNA
  x3dna-dssr -i=1jj2.pdb -o=1jj2.out  # large ribosomal subunit
  x3dna-dssr -i=5afi.cif -o=5afi.out  # ribosome (only in .cif)
  x3dna-dssr -i=5afi.cif -o=5afi-pairs.out --PAIR-ONLY  # 10x faster
  x3dna-dssr -i=1msy.pdb --json -o=1msy.json
     # x3dna-dssr -i=1msy.pdb --json | jq .pairs
  x3dna-dssr -i=5afi.cif --json --pair-only
  x3dna-dssr -i=2n2d.pdb --nmr --json -o=2n2d-dssr.json
  x3dna-dssr -i=1msy.pdb --blocview --block-file=wc -o=1msy.pml
     # load '1msy.pml' into PyMOL for interactive visualization
  x3dna-dssr -i=1msy.pdb --frame='A.2658-wc-minor' -o=1msy-bp.pdb
     # set 1msy into the minor-groove view of the C2658-G2663 pair
  x3dna-dssr -i=1oct.pdb --get-hbond  # H-bonds in DNA (default)
  x3dna-dssr -i=1oct.pdb --get-hbond=nuc+protein  # plus H-bonds in proteins
  x3dna-dssr snap -h  # help for the SNAP module on the interactions
                      #   of DNA-protein or RNA-protein complexes
```

The above help message should be sufficient to get most users started using DSSR. It is worth noting that the command-line interface is consistent on all operating systems, including the command shell on Windows.

DSSR introduces a consistent and flexible way to process command-line options. Here, each option can be specified via a `--key[=value]` pair, or `-key[=value]` or `key[=value]`; i.e., two/one/zero preceding dashes are all acceptable. The key can be in lower, UPPER or MiXed case, and the value is optional for Boolean switches. Moreover, options can be put in any order; if the same key is repeated more than once, the value specified with the last key prevails. Some typical use cases are given below:

```
#1 analyze the PDB entry '1msy', with default output to stdout
x3dna-dssr --input=1msy.pdb

#2 same as #1, with output directed to file '1msy.out'
x3dna-dssr --input=1msy.pdb --output=1msy.out
```

```
#3-6, same as #2
x3dna-dssr --output=1msy.out --input=1msy.pdb
x3dna-dssr --OUTPUT=1msy.out --Input=1msy.pdb
x3dna-dssr -output=1msy.out input=1msy.pdb
x3dna-dssr output=1msy.out --input=1msy.pdb

#7 the value '1ehz.pdb' overwrites '1msy.pdb'
x3dna-dssr --input=1msy.pdb input=1ehz.pdb

#8-12 with the switch --more set to true
x3dna-dssr -input=1msy.pdb --more
x3dna-dssr -input=1msy.pdb --more=true
x3dna-dssr -input=1msy.pdb --more=yes
x3dna-dssr -input=1msy.pdb --more=on
x3dna-dssr -input=1msy.pdb --more=1

#13 same as without specifying --more,
#      or with values set to false/no/0
x3dna-dssr -input=1msy.pdb --more=off

#14 shorthand forms for --input and --output
x3dna-dssr -i=1msy.pdb -o=1msy.out

#15 it can also be more verbose
x3dna-dssr --input-pdb-file=1msy.pdb

#16-19 within a key, separator dash(-) and underscore (_)
#      are treated the same, and can be omitted
x3dna-dssr -i=1msy.pdb -non-pair
x3dna-dssr -i=1msy.pdb -non_pair
x3dna-dssr -i=1msy.pdb -nonpair
x3dna-dssr -i=1msy.pdb -nonPair
```

By allowing for two/one/zero dashes to precede each key and a dash/underscore/none to separate words within a key, DSSR provides great versatility in specifying command-line options to fit into a user-preferred style.

3.2 Default run on PDB entry 1msy: detailed explanations

The PDB entry 1msy is a small RNA fragment with 27 nucleotides, containing a GUAA tetraloop (GNRA-type) mutant of the sarcin/ricin domain from *E. Coli* 23S rRNA[12] that includes a bulged-G motif (the GpU dinucleotide platform[13]). This structure contains several features that nicely illustrate fundamental aspects of DSSR.

Let the PDB-formatted 3D coordinate file be called `1msy.pdb` (as shown below, the PDBx/mmCIF version `1msy.cif` works as well), the output file `1msy.out`, and leave all other options in their default settings. Then simply run the command:

```
x3dna-dssr -i=1msy.pdb -o=1msy.out
x3dna-dssr -i=1msy.cif -o=1msy.out # gives the same results as above
```

The screen output provides a brief summary of the run, as shown below. Note that DSSR starts from a raw `.pdb` or `.cif` file as directly downloaded from the PDB, and takes little time to analyze small to mid-size (non-ribosomal) structures.

```
    total number of nucleotides: 27
    total number of base pairs: 13
    total number of helices: 1
    total number of stems: 1
    total number of isolated WC/wobble pairs: 1
    total number of multiplets: 1
    total number of atom-base capping interactions: 2
    total number of splayed-apart dinucleotides: 1
    total number of hairpin loops: 1
    total number of internal loops: 1
    total number of non-loop single-stranded segments: 2

Time used: 00:00:00:00
```

For easy reference, Figure 2 shows the 3D structure and the corresponding secondary (2D) structure of 1msy. The schematic 3D structure was automatically generated in schematic `blocview` representation. The 2D diagram was rendered with VARNA[7], using DSSR-generated 2D structure in connectivity table format (`.ct`, see below).

The main output file (`1msy.out`) contains many sections. We will go over them one by one, along the way, explaining the notations used therein. Additionally, DSSR generates the following auxiliary files (named with prefix `dssr-` by default):

```
List of 13 additional files
   1 dssr-pairs.pdb -- an ensemble of base pairs
   2 dssr-multiplets.pdb -- an ensemble of multiplets
   3 dssr-stems.pdb -- an ensemble of stems
   4 dssr-helices.pdb -- an ensemble of helices (coaxial stacking)
   5 dssr-hairpins.pdb -- an ensemble of hairpin loops
   6 dssr-iloops.pdb -- an ensemble of internal loops
   7 dssr-2ndstrs.bpseq -- secondary structure in bpseq format
   8 dssr-2ndstrs.ct -- secondary structure in connectivity table format
   9 dssr-2ndstrs.dbn -- secondary structure in dot-bracket notation
  10 dssr-torsions.txt -- backbone torsion angles and suite names
  11 dssr-splays.pdb -- an ensemble of splayed-apart units
  12 dssr-stacks.pdb -- an ensemble of base stacks
  13 dssr-atom2bases.pdb -- an ensemble of atom-base stacking interactions
```

3.2.1 Summary section

```
Note: By default, each nucleotide is identified by chainId.name#. So a
      common case would be B.A1689, meaning adenosine #1689 on chain B.
      One-letter base names for modified nucleotides are put in lower
      case (e.g., 'c' for 5MC). For further information about the output
      notation, please refer to the DSSR User Manual.
```

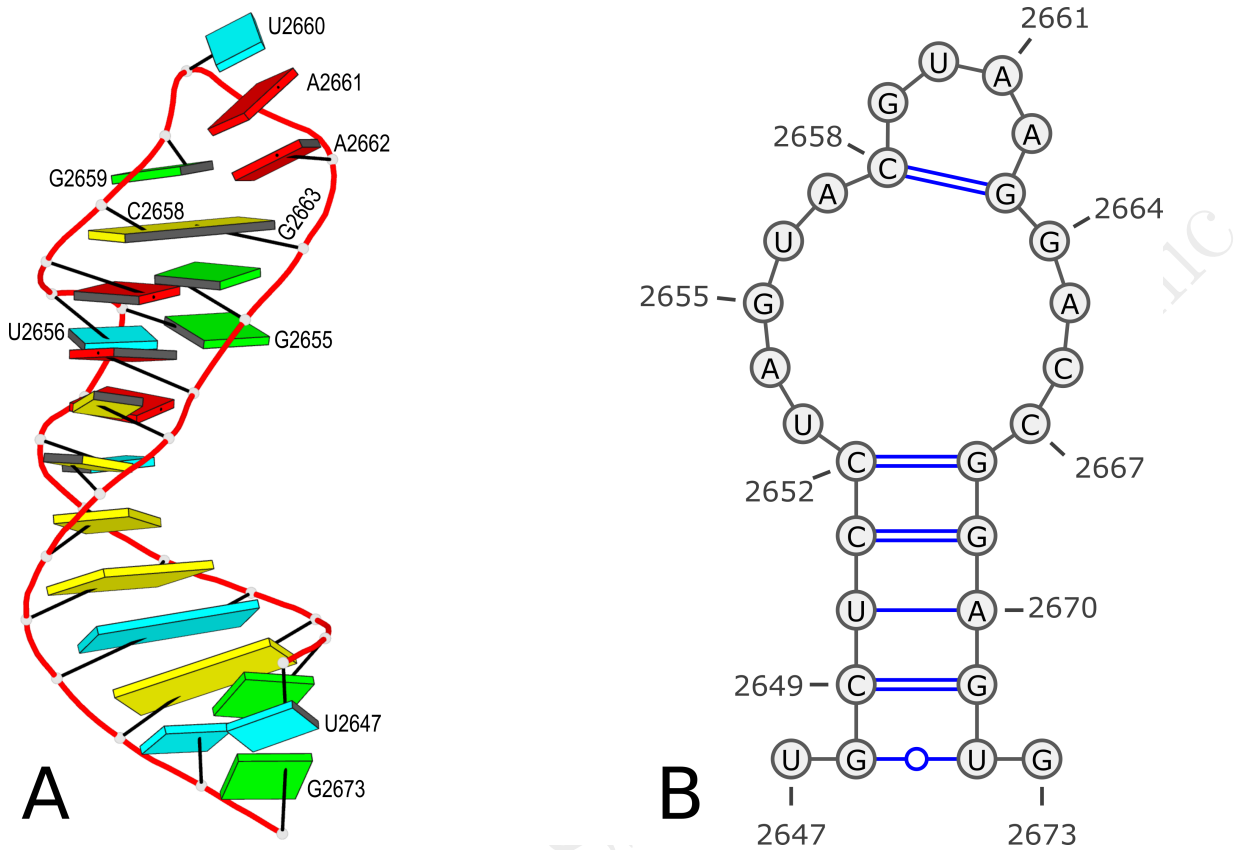

Figure 2: Images of PDB entry 1msy. (A) Schematic 3D structure in block presentation[3]. (B) 2D diagram produced with VARNA[7] using DSSR-derived secondary structure information in `.ct` format.

```
    Questions and suggestions are *always* welcome on the 3DNA Forum.

Command: x3dna-dssr -i=1msy.pdb -o=1msy.out
File name: 1msy.pdb
    no. of DNA/RNA chains: 1 [A=27]
    no. of nucleotides:    27
    no. of atoms:          685
    no. of waters:         109
    no. of metals:         0
```

The note in the summary section first explains how a nucleotide (nt) is specified in the output file. Typically, a chain id, residue name, and sequence number are sufficient to unambiguously specify a nt. For example, `A.G19` means guanosine no. 19 on chain A. In addition to the standard three-letter residue names commonly adopted (as in the PDB), DSSR also uses a one-letter shorthand symbol. For RNA, the four standard nts in three-letter form—␣␣A, ␣␣C, ␣␣G and ␣␣U (where ␣ stands for a space)—are shortened to A, C, G,

and U, respectively. For DNA, the three-letter (one-letter) nts are ⊔DA (A), ⊔DC (C), ⊔DG (G), and ⊔DT (T), respectively. The one-letter shorthand forms for modified nts, which occur frequently in RNA (e.g., tRNA), are mapped to their canonical counterparts, but put in lower case letters (e.g., c for 5MC). Note that pseudouridine, the most prevalent modified nt in RNA, is denoted P in DSSR and the small case p is reserved for potential modified pseudouridines.

The following sections provide more information on notations that are used consistently in DSSR output files. It is worth the time and effort to become familiar with them. In practice, a normal user should have little difficulty following the convention, after going over a few examples.

The remaining lines in the summary section should be self-explanatory. The `Command:` line provides the running DSSR command with relevant options so that the results can be reproduced. The meaning of the `Date and time:` line is obvious. The `File name:` line lists the data file analyzed by DSSR, followed by a list of numbers: DNA/RNA chains (here chain A with 27 nts), nts (27), atoms (685), waters (109), and metals (0). In cases with more than one chain or type of metal, the output would be as below (using 1jj2 as an example).

```
no. of DNA/RNA chains: 2 [0=2754,9=122]
no. of metals:         210 [Na=86,Mg=117,K=2,Cd=5]
```

Here the first line means that 1jj2 contains two RNA chains: 0 and 9, with 2754 and 122 nts, respectively. The second line indicates the PDB entry includes 210 metal atoms: 86 Na, 117 Mg, 2 K, and 5 Cd.

3.2.2 Base pairs

DSSR identifies a total of 13 bps, including not only the canonical Watson-Crick (WC) and wobble pairs, but also non-canonical bps (a dinucleotide platform, reverse Hoogsteen, sheared G–A, etc.).

```
List of 13 base pairs
     nt1            nt2            bp  name         Saenger   LW   DSSR
   1 A.U2647        A.G2673        U-G --           --        cWW  cW-W
   2 A.G2648        A.U2672        G-U Wobble       28-XXVIII cWW  cW-W
   3 A.C2649        A.G2671        C-G WC           19-XIX    cWW  cW-W
   4 A.U2650        A.A2670        U-A WC           20-XX     cWW  cW-W
   5 A.C2651        A.G2669        C-G WC           19-XIX    cWW  cW-W
   6 A.C2652        A.G2668        C-G WC           19-XIX    cWW  cW-W
   7 A.U2653        A.C2667        U-C --           --        tW.  tW-.
   8 A.A2654        A.C2666        A+C --           --        tHH  tM+M
   9 A.G2655        A.U2656        G+U Platform     --        cSH  cm+M
  10 A.U2656        A.A2665        U-A rHoogsteen   24-XXIV   tWH  tW-M
```

```
  11 A.A2657        A.G2664        A-G Sheared     11-XI     tHS  tM-m
  12 A.C2658        A.G2663        C-G WC          19-XIX    cWW  cW-W
  13 A.G2659        A.A2662        G-A Sheared     11-XI     tSH  tm-M
```

As the header line (the 2nd in the listing) shows, each bp is characterized by the two constituent nts (nt1 and nt2), and an abbreviated bp type of the form M±N. Here M and N are the one-letter shorthand symbol of the nts, which can be in upper or lower cases (for modified nts), as noted above. The symbol ± reflects the two possible relative 'face' orientations between the two planar base moieties: the sign is normally − as for canonical WC/wobble bps with opposite faces, and + if one of the two base planes is *flipped*. Figure 3 provides further details on the rationale of the M±N convention[13] that is used consistently in 3DNA[9,10] and DSSR[1].

The name column gives the common names of the corresponding bps, where appropriate. Currently, the list includes WC, reverse WC (rWC), Hoogsteen, reverse Hoogsteen (rHoogsteen), wobble, sheared, imino, Calcutta, and dinucleotide platform, and unnamed bps are designated `--`. Other than WC and wobble pairs, the PDB entry 1msy also contains a GpUpA/GpA miniduplex[13] characterized by three common bps (nos. 9 to 11): a platform (G+U), a reverse Hoogsteen (U–A), and a sheared (A–G). However, it is difficult to connect those bp structures with their familiar names, even for experts. With DSSR-assigned names, one can immediately see common bps and their types within a structure. As it turns out, the name column is also handy to quickly delineate stretches of canonical pairs (e.g., nos 2 to 6 in the listing on Page 13) that form double-helical regions, termed 'stem' in DSSR (see Page 23).

The Saenger column provides the classification of 29 bp types with at least two H-bonds between base atoms. This list, initially compiled by Saenger for 28 bps[5], includes an extra G+C bp added to the list by Burkard *et al.* in an appendix to the second edition of "The RNA World" book[14]. Note that in addition to the Roman numerals (I to XXIX) originally used by Saenger, the DSSR output also includes the corresponding Arabic numerals (01 to 29), which may be easier for some users to recognize (at least for myself). If a pair cannot be categorized into one of the 29 known types, the symbol `--` is assigned.

The LW column in the list of base pairs (on Page 13) gives Leontis-Westhof classification of bps[6]. As illustrated in Figure 4 (see below), this classification is based on the three edges of each base with potential for H-bonding interactions (Watson-Crick, Hoogsteen, and Sugar), and the two orientations (*cis* or *trans*) of the interacting bases with respect to the glycosidic bonds. The combinations of edges and orientations "gives rise to 12 basic geometric types with at least two H bonds connecting the bases"[6]. This geometry-based method captures

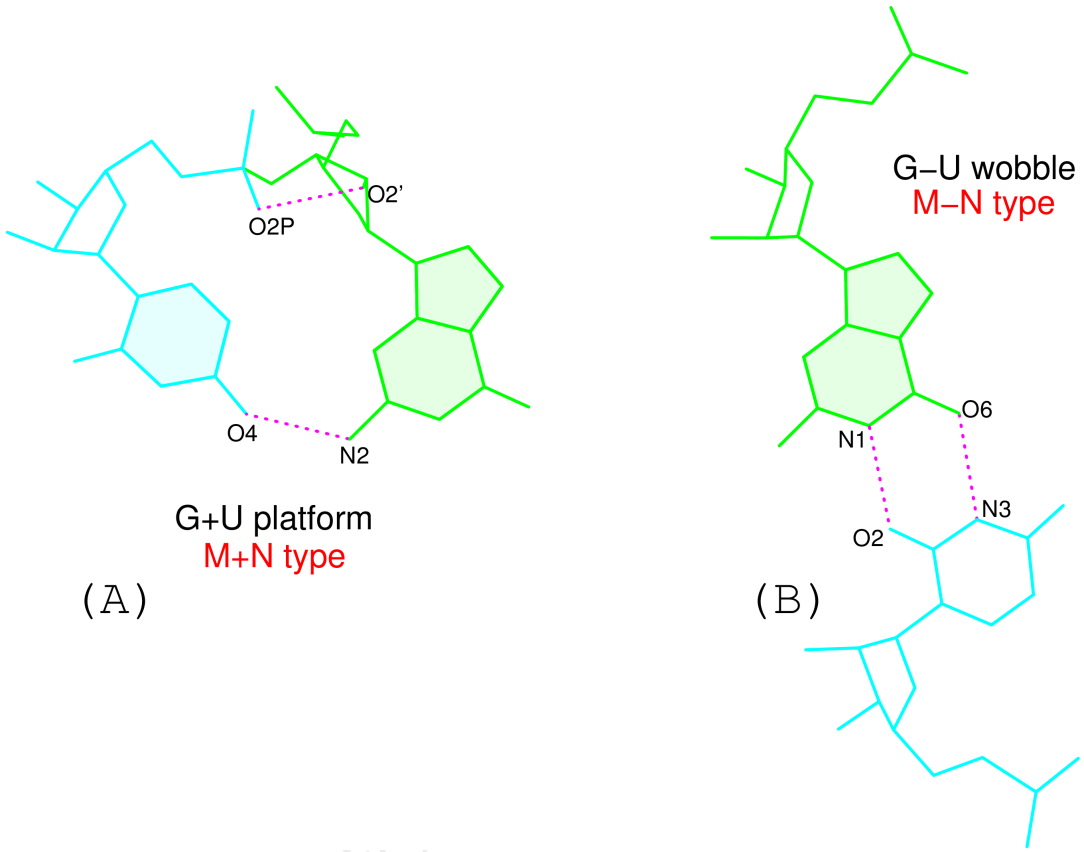

Figure 3: Comparison of the parallel M+N and antiparallel M–N arrangements of G and U bases found in (A) the G+U platform and (B) the G–U wobble pair, respectively. Here G is depicted in green, and U in cyan. For easy comparison, the two pairs are oriented in the standard reference frame of the guanine base, with the shading used to specify the face from which the positive base normal, i.e., *z*-axis, emanates. The U shares the same face as G in the G+U dinucleotide platform (A); the *z*-axes of the two bases are parallel, forming a positive dot product expected of M+N pairing. By contrast, the U points in the opposite direction from G in the G–U wobble pair (B); the *z*-axes of the two bases are anti-parallel, forming a negative dot product expected of M–N pairing. Note that this M–N nomenclature follows the convention expected for the canonical, antiparallel Watson-Crick base pairs: A–U/A–T and G–C.

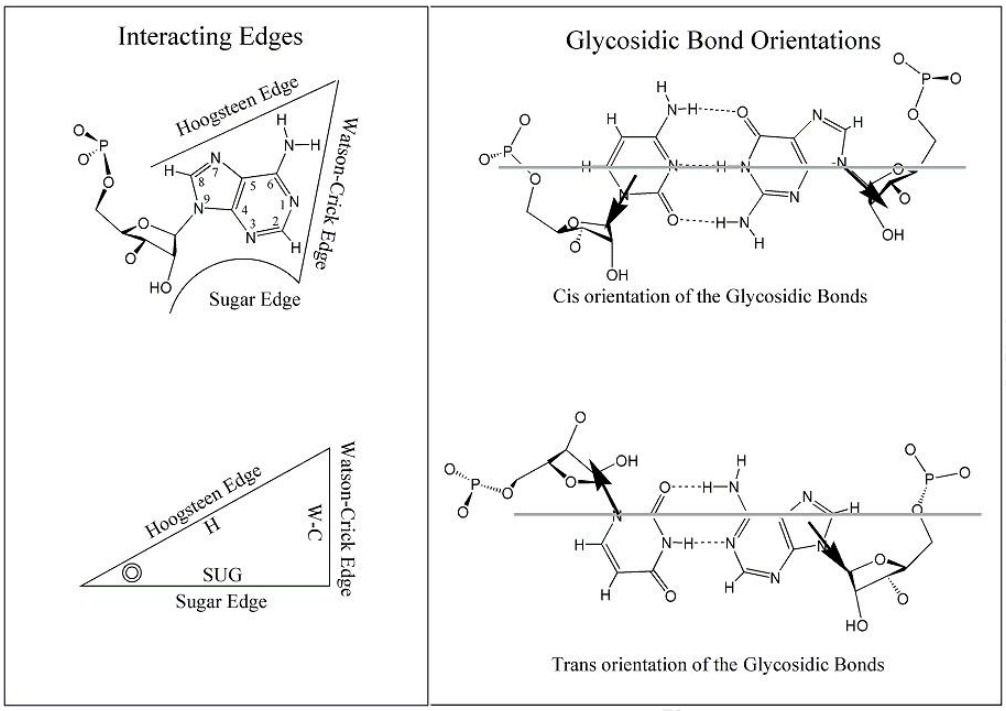

Figure 4: Base edges and base-pair geometric isomerism. (Upper left) An adenosine showing the three base edges (Watson-Crick, Hoogsteen, and Sugar-edge) available for H-bonding interactions. (Lower left) Representation of an RNA base as a triangle. The position of the ribose is indicated with a circle in the corner defined by the Hoogsteen and Sugar edges. (Right) *Cis* and *trans* base-pairing geometries, illustrated for two bases interacting with Watson-Crick edges[6].

salient features of bp interactions and strikes a balance between simplicity and expressiveness. The LW scheme is more generally applicable than the Saenger classification, and it is easy to grasp by biologists. As a result, the LW bp classification has become standard in RNA structural bioinformatics.

Strictly speaking, however, the RNA-centric LW classification has its limitations (Figure 5). For one thing, the Sugar edge explicitly includes the 2′-hydroxyl group, rendering it less applicable to DNA structures. Moreover, while the aromatic base can be taken as a rigid body with three fixed edges, the χ (chi) torsion angle characterizes the internal freedom between base and sugar (*anti*/*syn*). When χ is in the relatively rare but by no means uncommon *syn* conformation, the Sugar edge, defined by the common *anti* conformation, no longer seems to exist.

The rich variety of RNA bps extends beyond the 12 basic LW types. There are numerous

pairs in RNA with only one H-bond or with bifurcated H-bonds, at boundary locations where the LW classification does not strictly apply. Lemieux and Major[15] were the first to extend the LW nomenclature. We noted the importance of the out-of-plane 'backbone edge' formed by an RNA-specific H-bond between O2′(G) and OP2(U)[13]. The RNA 3D Hub website, hosted by the Leontis-Zirbel co-lab, lists non-standard bp interactions ncSW, ntSH, and ntHH for the 1msy entry.

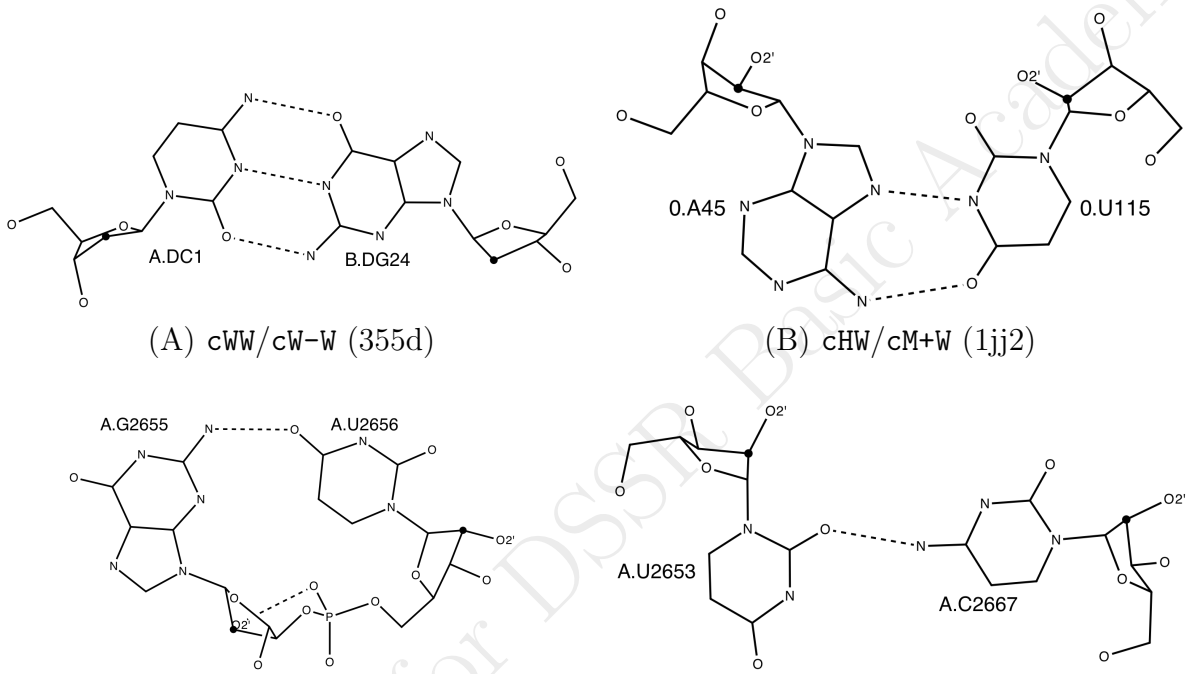

(A) `cWW/cW-W` (355d) (B) `cHW/cM+W` (1jj2)

(C) `cSH/cm+M` (1msy) (D) `tW./tW-.` (1msy)

Figure 5: Sample cases where the Leontis-Westhof definition of the three edges does not strictly apply. The results of LW/DSSR classifications are those implemented in the DSSR program. In each image, H-bonds are shown as dashed lines, C2′ atoms in black dots, and O2′ atoms labeled. (A) A Watson-Crick C–G pair in 355d, a standard B-DNA molecule. The sugar-edge for C or G does not have an O2′ atom. (B) The Hoogsteen A+U pair in 1jj2. Here, nucleotide 0.A45 is in the *syn* conformation; thus the O2′ atom is pointing away from (instead of towards) the minor-groove edge of the base. (C) The G+U platform (in 1msy) has an out-of-plane 'backbone edge'. (D) The U–C pair (in 1msy) has only one boundary H-bond. Thus, the interacting edge for A.C2667 cannot be unambiguously assigned.

The DSSR bp classification is presented in the last column (e.g., `cW-W` for canonical bps, and `cm+M` for the G+U dinucleotide platform). Overall, the DSSR scheme follows the

pattern of `[ct][WMm]±[WMm]` (see Figure 1C). Here, `[ct]` stands for *cis*/*trans*, defined by the positioning of the glycosidic bonds related to a line connecting the centers of base-ring atoms; `[WMm]` for the interacting edges defined with reference to an idealized WC bp: W for the Watson-Crick edge, M for the Major-groove edge, m for the minor-groove edge; ± for normal (−) *vs.* flipped (+) base orientations, as noted above. The dot symbol denotes cases where edges or orientations cannot be defined (see bp no. 7 in the list of base pairs on Page 13, and Figure 5(D)).

In general, the M in DSSR scheme corresponds to the Hoogsteen/CH-edge (H) in the LW notation, and the m to the LW Sugar-edge (S) if χ is in the *anti* conformation. In the DSSR implementation, we assumes direct correspondences between M/H, and m/S, regardless of the *anti*/*syn* base-sugar orientations. Moreover, the LW *cis*/*trans* is assigned in the same way as for the DSSR scheme. So the LW and DSSR notations are strictly parallel, excerpt for the extra ± character in the DSSR classification.

The M±N bp notation has been used consistently in 3DNA for over a decade, and a whole section titled 'Base pair parameters' is included in the 2003 3DNA publication[9]. The orientation, combined with the six standard bp parameters (shear, stretch, stagger, buckle, propeller, and opening; see Figure 7) derived from the 3DNA `analyze` program, can unambiguously characterize any pair. Conversely, given the M±N notation with six corresponding bp parameters, the 3DNA `rebuild` program can rigorously reconstruct the spatial disposition of the two interacting bases. This reversibility is one of the unique features of 3DNA and can be applied to bps in both DNA and RNA.

Even with the increasing popularity of 3DNA, the value of using M±N with six parameters to classify bps has never received the attention it deserves, especially in the RNA structural bioinformatics community. The incorporation of bp classifications in DSSR provides an opportunity to emphasize the strength of this approach. In DSSR, the three interacting edges strictly center on a base, which can be taken as a *rigid* body. The standard base reference frame[4] has distinct geometric features to allow for easy identification of the edges (Figure 1C). As is also clear from Figure 1C, for WC pairs, the distinction of the minor-groove vs. the major-groove edges is simply a consequence of the asymmetric glycosidic linkage between the base and sugar moiety. Moreover, the terminology of minor/major grooves is widely used, even in the RNA structure literature: the most obvious being the A-minor motif[16] (see Section 3.4.2).

Our recent paper "Effects of noncanonical base pairing on RNA folding: structural context and spatial arrangements of G·A pairs"[17] in the ACS *Biochemistry* journal highlights the advantages enabled by DSSR to uncover previously unrecognized patterns. The key features

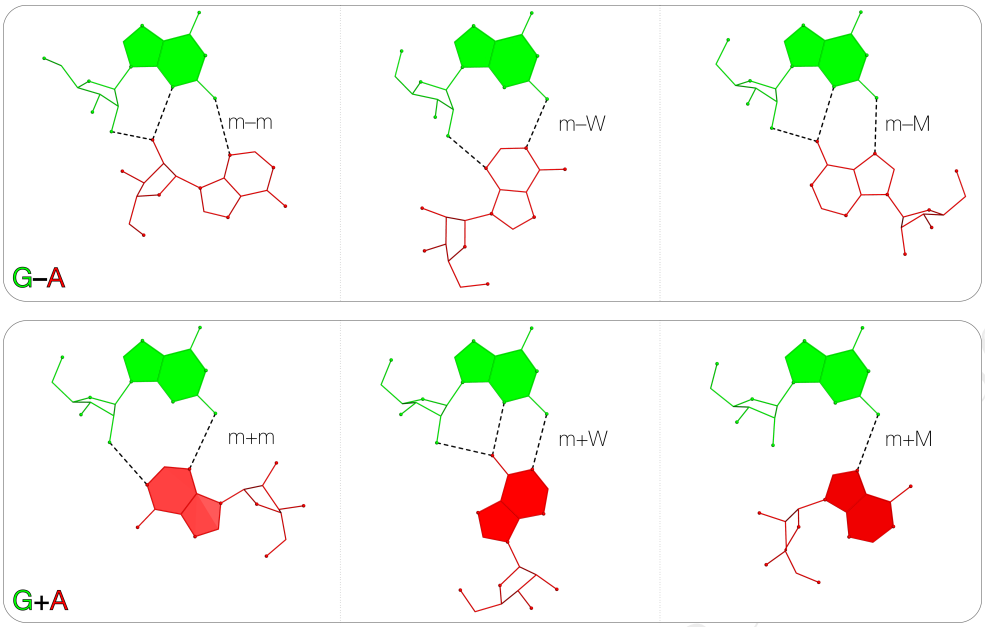

Figure 6: Six types of G·A pairs, uncovered and characterized by DSSR, that involve the minor-groove edge of G. Top row: three examples in the G–A category with types m–m, m–W, and m–M, respectively; Bottom row: three cases in the G+A category with types m+m, m+W, and m+M, respectively.

are summarized in the abstract (see Figure 6), and excerpted below:

> "The rigorous descriptions of base-pair geometry that we employ facilitate characterization of recurrent geometric motifs and the structural settings in which these arrangements occur. Moreover, the numerical parameters hint at the natural motions of the interacting bases and the pathways likely to connect different spatial forms. We draw attention to higher-order multiplexes involving two or more G·A pairs and the roles these associations appear to play in bridging different secondary structural units."

DSSR also produces a file named `dssr-pairs.pdb` that contains an ensemble of MODEL/ENDMDL delineated atomic coordinates for identified bps. Each bp is expressed in its own reference frame for easy and consistent visualization.

3.2.3 Multiplets (higher-order coplanar base associations)

There is only one multiplet, a triplet, in 1msy, as shown below.

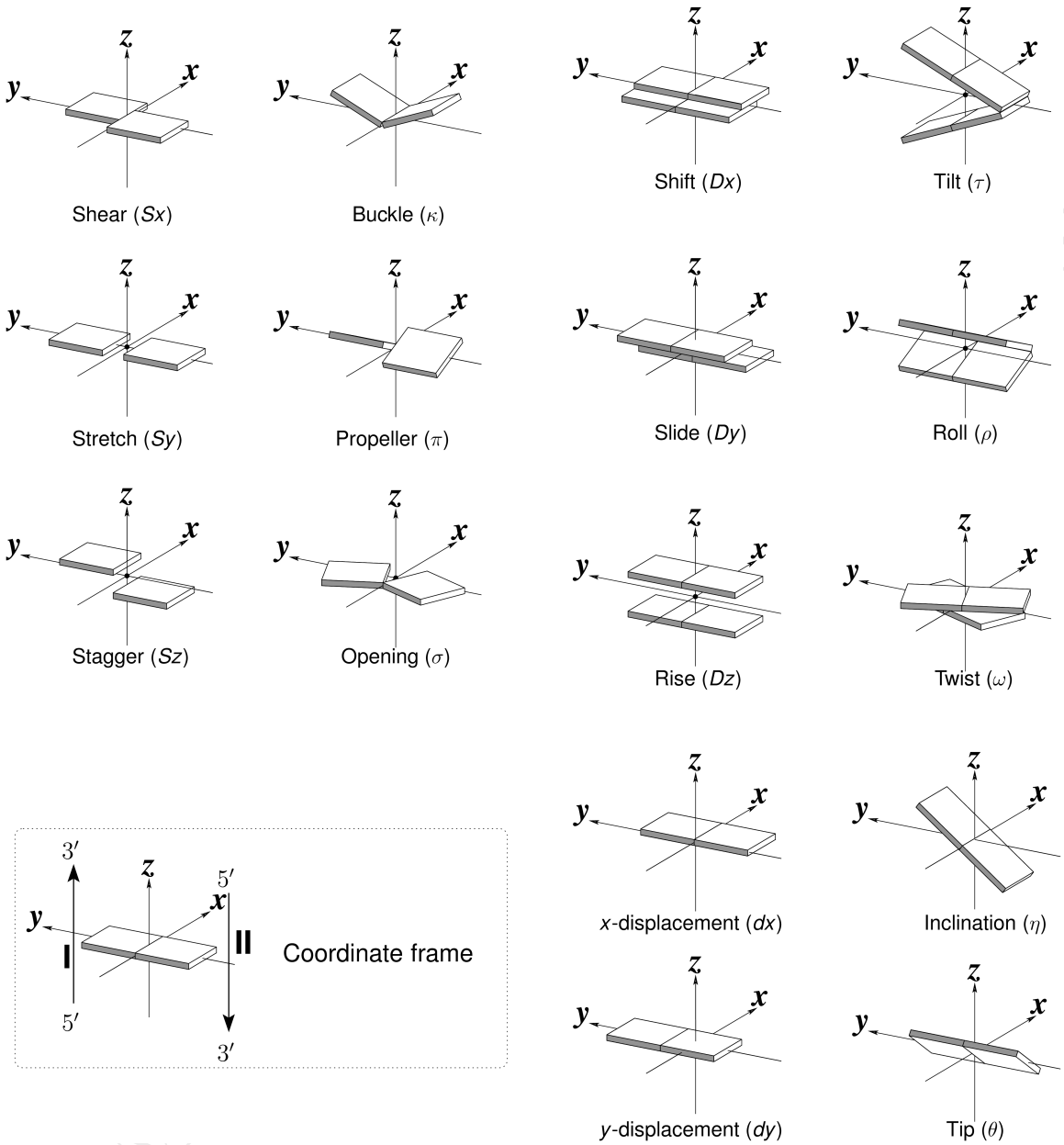

Figure 7: Pictorial definitions of rigid-body parameters used to describe the geometry of complementary (or non-complementary) base pairs and sequential base pair steps. The base-pair reference frame (lower left) is constructed such that the x-axis points away from the (shaded) minor groove edge of a base or base pair and the y-axis points toward the sequence strand (I). The relative position and orientation of successive base pair planes are described with respect to both a dimer reference frame (upper right) and a local helical frame (lower right). Images illustrate positive values of the designated parameters.

```
List of 1 multiplet
   1 nts=3 GUA A.G2655,A.U2656,A.A2665
```

For each identified multiplet, the serial number (1) is followed by the number of nts (3), the base sequence in one-letter shorthand form (GUA), and a comma-delimited list of the corresponding nts. The G-tetrad motif, which forms the G-quadruplexes, is also detected with DSSR (although not in 1msy); it is simply a special multiplet with four Gs.

As for bps, DSSR also generates a file (named `dssr-multiplets.pdb` by default) for MODEL/ENDMDL delineated multiplets. In the file, each multiplet is set to the most extended view with respect to the base rings. The triplet in 1msy is shown in Figure 8. Note the extensive network of H-bonding interactions between the three nts[13].

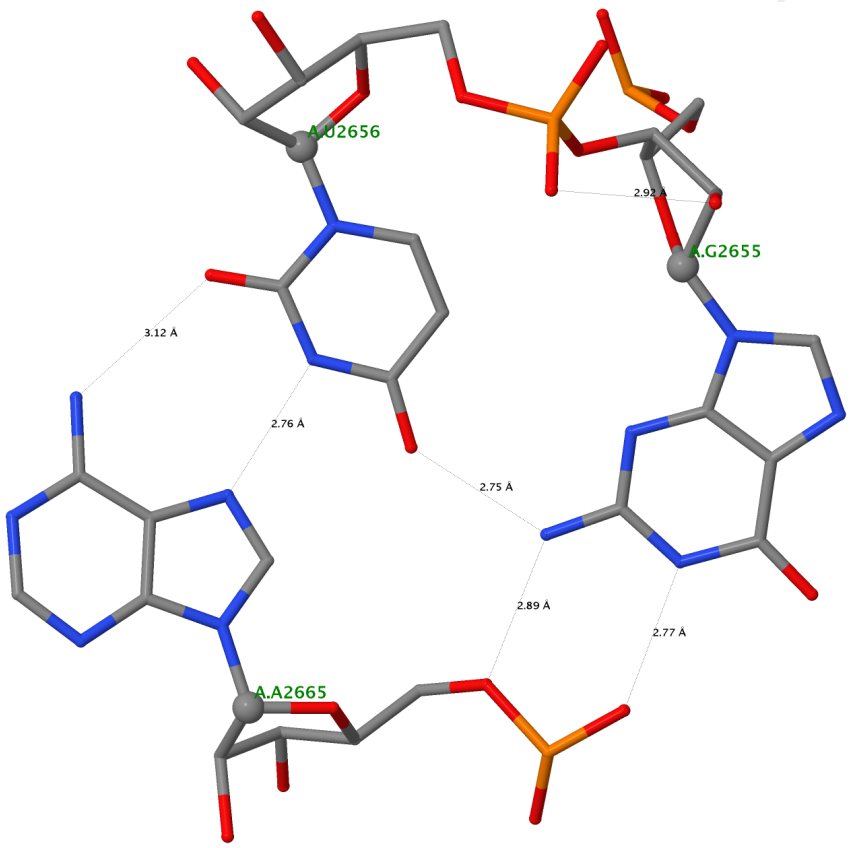

Figure 8: The GUA triplet identified in 1msy. Here G2655 and U2656 form a G+U dinucleotide platform; U2656 and A2665 form a reverse Hoogsteen pair. The phosphate group of A2665 interacts with the Watson-Crick edge of G2655 with two sequence-specific H-bonds. The image was produced with Jmol.

3.2.4 Helices

DSSR identifies one helix with 12 bps in 1msy (see below). This section starts with a note explaining the definition of a helix, and other related information. By referring to Figure 2(A), one can immediately see the duplex formed by base-stacking interactions, starting from the very bottom of the structure all the way up to the sheared G–A pair at the top (part of the GUAA tetraloop). Note that by definition, a helix is composed of at least two stacked bps.

```
List of 1 helix
  Note: a helix is defined by base-stacking interactions, regardless of bp
        type and backbone connectivity, and may contain more than one stem.
      helix#number[stems-contained] bps=number-of-base-pairs in the helix
      bp-type: '|' for a canonical WC/wobble pair, '.' otherwise
      helix-form: classification of a dinucleotide step comprising the bp
        above the given designation and the bp that follows it. Types
        include 'A', 'B' or 'Z' for the common A-, B- and Z-form helices,
        '.' for an unclassified step, and 'x' for a step without a
        continuous backbone.
      ------------------------------------------------------------------
  helix#1[1] bps=12
      strand-1 5'-UGCUCCUAUACG-3'
       bp-type    .|||||....|.
      strand-2 3'-GUGAGGCCAGGA-5'
      helix-form  ..AAA..x...
   1 A.U2647        A.G2673        U-G --            --        cWW  cW-W
   2 A.G2648        A.U2672        G-U Wobble        28-XXVIII cWW  cW-W
   3 A.C2649        A.G2671        C-G WC            19-XIX    cWW  cW-W
   4 A.U2650        A.A2670        U-A WC            20-XX     cWW  cW-W
   5 A.C2651        A.G2669        C-G WC            19-XIX    cWW  cW-W
   6 A.C2652        A.G2668        C-G WC            19-XIX    cWW  cW-W
   7 A.U2653        A.C2667        U-C --            --        tW.  tW-.
   8 A.A2654        A.C2666        A+C --            --        tHH  tM+M
   9 A.U2656        A.A2665        U-A rHoogsteen    24-XXIV   tWH  tW-M
  10 A.A2657        A.G2664        A-G Sheared       11-XI     tHS  tM-m
  11 A.C2658        A.G2663        C-G WC            19-XIX    cWW  cW-W
  12 A.G2659        A.A2662        G-A Sheared       11-XI     tSH  tm-M
```

Of the 13 bps listed on Page 13, only the G+U dinucleotide platform formed by G2655 and U2656 is not contained in the helix. Since U2656 also forms a reverse Hoogsteen U–A pair with A2665 (as part of the triplet, see Figure 8), and the U–A bp is included in the helix, only the so-called bulged G (i.e., G2655) is excluded.

The helix-form subsection (lines with `strand-1`, `by-type`, `strand-2`, and `helix-form`, respectively) gives a quick summary of the stacked bps: base sequences, bp types (canonical or otherwise), and helix conformations of the dinucleotide steps. Needless to say, the A-form helix is the most common type for RNA. However, since DSSR can be equally applied to DNA, the B- and Z-forms would also be included in the classification.

3.2.5 Stems (canonical pairs with continuous backbones)

In DSSR, a stem is defined as a helix consisting of only canonical WC/wobble pairs and possessing a continuous backbone along each strand. The literature does not appear to be consistent as to what constitutes a helix, stem, or arm. Hopefully DSSR will help to clarify the confusion in the field. The default requirement for canonical bps in DSSR follows the convention widely adopted for RNA secondary structures, as in the mfold/UNAFold software and the ViennaRNA Package. The PDB entry 1msy contains one stem with five canonical bps, as shown below (see also Figure 2(B)). Notice how the bp names and the helix-form sub-section on Page 22 facilitate a quick visual identification of the stem in the helix.

```
List of 1 stem
  Note: a stem is defined as a helix consisting of only canonical WC/wobble
        pairs, with a continuous backbone.
      stem#number[#helix-number containing this stem]
      Other terms are defined as in the above Helix section.
      ------------------------------------------------------------------
  stem#1[#1] bps=5
      strand-1 5'-GCUCC-3'
       bp-type    |||||
      strand-2 3'-UGAGG-5'
      helix-form  .AAA
   1 A.G2648        A.U2672        G-U Wobble        28-XXVIII cWW  cW-W
   2 A.C2649        A.G2671        C-G WC            19-XIX    cWW  cW-W
   3 A.U2650        A.A2670        U-A WC            20-XX     cWW  cW-W
   4 A.C2651        A.G2669        C-G WC            19-XIX    cWW  cW-W
   5 A.C2652        A.G2668        C-G WC            19-XIX    cWW  cW-W
```

3.2.6 Isolated canonical pairs

DSSR defines an isolated canonical bp as the one that is not part of a stem. In 1msy, `A.C2658` and `A.G2663` form such an isolated C–G WC pair, as detailed below. The `[#1]` at the beginning means this pair is part of helix #1. Note also the negative indices for isolated canonical bps vs. the positive values for stems. The significance of the distinction will become obvious later on, as internal and hairpin loops are specified.

```
List of 1 isolated WC/wobble pair
  Note: isolated WC/wobble pairs are assigned negative indices to
        differentiate them from the stem numbers, which are positive.
        ---------------------------------------------------------------
[#1]     -1 A.C2658        A.G2663        C-G WC            19-XIX    cWW  cW-W
```

3.2.7 Base stacks

DSSR defined a base stack as an ordered list of nucleotides assembled together via base-stacking interactions, regardless of backbone connectivity or pairing involvement. Stacking interactions within a stem are **not** included by default. In 1msy, note the UAA stack (no. 2 in the listing) in the GUAA tetraloop, and the GGGG stack (no. 4). See Figure 2. Nucleotides not involved in stacking interactions are also listed, if any.

```
List of 5 base stacks
  Note: a stack is an ordered list of nucleotides assembled together via
        base-stacking interactions, regardless of backbone connectivity.
        Stacking interactions within a stem are *not* included.
   1 nts=2 GG A.G2648,A.G2673
   2 nts=3 UAA A.U2660,A.A2661,A.A2662
   3 nts=4 CUAU A.C2652,A.U2653,A.A2654,A.U2656
   4 nts=4 GGGG A.G2655,A.G2664,A.G2663,A.G2659
   5 nts=6 CAACCG A.C2658,A.A2657,A.A2665,A.C2666,A.C2667,A.G2668
```

3.2.8 Atom-base capping interactions

First described by Quigley and Rich in the tRNA^{Phe} structure[18], the phosphate group (actually the exocyclic OP2 atom) can stack over a base ring to cap a helix. Atom-base capping interactions are often observed in other structural motifs, including U-turns or GNRA tetraloops.

In DSSR, the stacking atoms also includes oxygen from water or the sugar moiety. The output for 1msy is given below. Check also the associated PDB file `dssr-a2bases.pdb` to visualize the findings.

```
List of 2 atom-base capping interactions
    dv: vertical distance of the atom above the nucleotide base
    ------------------------------------------------------------
     type       atom                  nt              dv
   1 phosphate  OP2@A.A2661           A.G2659         3.04
   2 sugar      O4'@A.G2664           A.G2663         3.48
```

Here the `type` column can be ‘phosphate’, ‘sugar’, or ‘other’. The meaning of the `atom` and `nt` columns should be obvious. As noted on the 2nd line, the `dv` column gives vertical distance (in Å) of the atom from the nucleotide base. Thus, the first case shows that the OP2 atom of the A2661 phosphate group stacks 3.04 Å over the G2659 base ring.

3.2.9 Various loops

Commonly occurring RNA loops are illustrated in Figure 9. DSSR identifies all of these different types and further distinguishes symmetric vs. asymmetric internal loops.

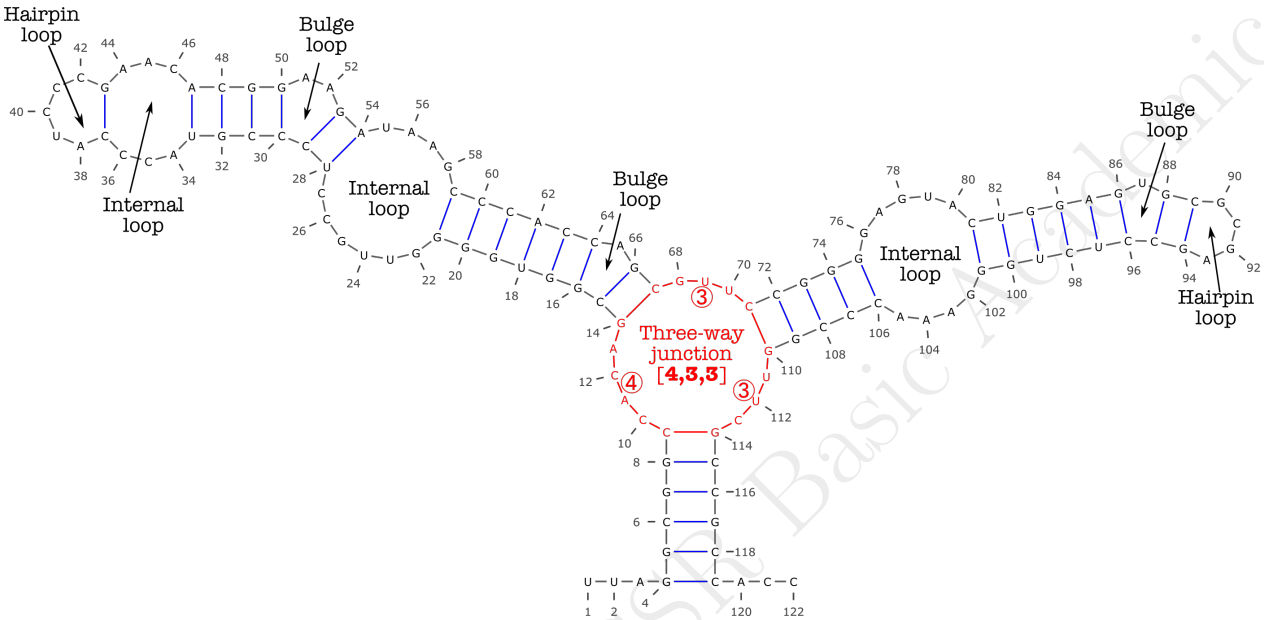

Figure 9: Common 2D structural elements of RNA. Single-stranded fragments at the 5′ and 3′ ends, and double-helical stems are obvious. 'Closed' loops of various types (hairpin, bulge, internal, and junction loops) are labeled.

DSSR finds one hairpin loop and an asymmetric internal loop in 1msy, as detailed below. Note that the list of the 13 nts in the internal loop is too long to fit on the page width. The list is actually written on the same line as `nts=13 CUAGUACGGACCG`.

```
Note: for the various types of loops listed below, numbers within the first
      set of brackets are the number of loop nts, and numbers in the second
      set of brackets are the identities of the stems (positive number) or
      isolated WC/wobble pairs (negative numbers) to which they are linked.

****************************************************************************
List of 1 hairpin loop
   1 hairpin loop: nts=6; [4]; linked by [#-1]
     summary: [1] 4 [A.2658 A.2663] 1
     nts=6 CGUAAG A.C2658,A.G2659,A.U2660,A.A2661,A.A2662,A.G2663
       nts=4 GUAA A.G2659,A.U2660,A.A2661,A.A2662

****************************************************************************
List of 1 internal loop
   1 asymmetric internal loop: nts=13; [5,4]; linked by [#1,#-1]
     summary: [2] 5 4 [A.2652 A.2668 A.2658 A.2663] 5 1
```

```
    nts=13 CUAGUACGGACCG A.C2652,A.U2653,A.A2654,A.G2655,A.U2656,A.A2657,A.C2658,A.G2663,A.
        ↪ G2664,A.A2665,A.C2666,A.C2667,A.G2668
      nts=5 UAGUA A.U2653,A.A2654,A.G2655,A.U2656,A.A2657
      nts=4 GACC A.G2664,A.A2665,A.C2666,A.C2667
```

With the note at the top and by referring to Figure 2(B), it should be straightforward to understand the meaning of most of the items in this section. Nevertheless, the two sets of matched brackets are worth further explanation. The hairpin loop contains a total of 6 nts, including the closing canonical pair: the `[4]` means 4 nts, i.e., a tetraloop; the `[#-1]` indicates that the tetraloop is closed by the first isolated pair. The asymmetric internal loop contains 13 nts in total: the `[5,4]` means 5 nts along one strand, and 4 nts on the other; `[#1,#-1]` indicates that the internal loop is linked by the first stem and the first isolated pair.

3.2.10 Single-stranded fragments

DSSR also characterizes single-stranded fragments not included in various loop regions. For 1msy, there are two, each consisting of one terminal nucleotide (see also Figure 2(B)).

```
List of 2 non-loop single-stranded segments
   1 nts=1 U A.U2647
   2 nts=1 G A.G2673
```

3.2.11 2D structure in dot-bracket notation

The DSSR-derived 2D structure is written in an extended dot-bracket notation (dbn) with information for pseudoknots (as matched `[]`, {}, or `<>` pairs, etc) and chain breaks (as `&`s), which can be fed directly into VARNA[7]. The dbn is written in FASTA format where the title line (with a `>` on the first column) is followed by base sequence and the 2D structure, each on a separate line. The dbn for 1msy is as follows.

```
Secondary structures in dot-bracket notation (dbn) as a whole and per chain
>1msy nts=27 [whole]
UGCUCCUAGUACGUAAGGACCGGAGUG
.(((((.....(....)....))))).
>1msy-A #1 nts=27 0.30(2.47) [chain] RNA
UGCUCCUAGUACGUAAGGACCGGAGUG
.(((((.....(....)....))))).
```

Since 1msy contains only a single continuous chain, the dbn contents for the whole and per chain are the same. For the Dickerson DNA dodecamer[19] structure 355d, the difference in contents between the whole structure and each chain is obvious from the directions of the

brackets (see below).

```
Secondary structures in dot-bracket notation (dbn) as a whole and per chain
>355d nts=24 [whole]
CGCGAATTCGCG&CGCGAATTCGCG
((((((((((((&))))))))))))
>355d-A #1 nts=12 3.21(0.51) [chain] DNA
CGCGAATTCGCG
((((((((((((
>355d-B #2 nts=12 3.37(0.50) [chain] DNA
CGCGAATTCGCG
))))))))))))
```

DSSR also generates a file named `dssr-2ndstrs.dbn` containing the 2D structure for the whole molecule in dbn notation. For better connection to third-party tools, DSSR produces an additional file named `dssr-2ndstrs.ct`, which expresses the 2D structure in connectivity table (`.ct`) format. First introduced by the mfold program, the `.ct` format is one of the most commonly used RNA 2D structure formats. The `.ct` output file for 1msy is listed below. Moreover, DSSR also generates a 2D structure representation in the `.bpseq` format in a file named `dssr-2ndstrs.bpseq`.

```
   27 ENERGY = 0.0 [1msy] -- secondary structure derived by DSSR
    1 U     0     2     0  2647 # name=A.U2647
    2 G     1     3    26  2648 # name=A.G2648, pairedNt=A.U2672
    3 C     2     4    25  2649 # name=A.C2649, pairedNt=A.G2671
    4 U     3     5    24  2650 # name=A.U2650, pairedNt=A.A2670
    5 C     4     6    23  2651 # name=A.C2651, pairedNt=A.G2669
    6 C     5     7    22  2652 # name=A.C2652, pairedNt=A.G2668
    7 U     6     8     0  2653 # name=A.U2653
    8 A     7     9     0  2654 # name=A.A2654
    9 G     8    10     0  2655 # name=A.G2655
   10 U     9    11     0  2656 # name=A.U2656
   11 A    10    12     0  2657 # name=A.A2657
   12 C    11    13    17  2658 # name=A.C2658, pairedNt=A.G2663
   13 G    12    14     0  2659 # name=A.G2659
   14 U    13    15     0  2660 # name=A.U2660
   15 A    14    16     0  2661 # name=A.A2661
   16 A    15    17     0  2662 # name=A.A2662
   17 G    16    18    12  2663 # name=A.G2663, pairedNt=A.C2658
   18 G    17    19     0  2664 # name=A.G2664
   19 A    18    20     0  2665 # name=A.A2665
   20 C    19    21     0  2666 # name=A.C2666
   21 C    20    22     0  2667 # name=A.C2667
   22 G    21    23     6  2668 # name=A.G2668, pairedNt=A.C2652
   23 G    22    24     5  2669 # name=A.G2669, pairedNt=A.C2651
   24 A    23    25     4  2670 # name=A.A2670, pairedNt=A.U2650
   25 G    24    26     3  2671 # name=A.G2671, pairedNt=A.C2649
   26 U    25    27     2  2672 # name=A.U2672, pairedNt=A.G2648
   27 G    26     0     0  2673 # name=A.G2673
```

3.2.12 Structural features per nucleotide

This section summarizes structural features that each nucleotide possesses or is part of. For each identified nucleotide, the output includes one-letter shorthand name, dbn, residue identifier, the rmsd of the base ring atoms, and a comma-separated list of features: *anti* or *syn* (χ) orientation, C2′ or C3′-endo sugar puckering, BI or BII backbone, modified or not, if involved in canonical or non-canonical pair, multiplet, helix, stem, or various loops, etc.

```
Summary of structural features of 27 nucleotides
  Note: the first five columns are: (1) serial number, (2) one-letter
    shorthand name, (3) dbn, (4) id string, (5) rmsd (~zero) of base
    ring atoms fitted against those in a standard base reference
    frame. The sixth (last) column contains a comma-separated list of
    features whose meanings are mostly self-explanatory, except for:
      turn: angle C1'(i-1)--C1'(i)--C1'(i+1) < 90 degrees
      break: no backbone linkage between O3'(i-1) and P(i)
   1  U . A.U2647   0.011  anti,~C3'-endo,non-canonical,non-pair-contact,helix-end,ss-non-loop
   2  G ( A.G2648   0.012  anti,~C3'-endo,BI,canonical,non-pair-contact,helix,stem-end
   3  C ( A.C2649   0.019  anti,~C3'-endo,BI,canonical,non-pair-contact,helix,stem
   4  U ( A.U2650   0.019  anti,~C3'-endo,BI,canonical,non-pair-contact,helix,stem
   5  C ( A.C2651   0.024  anti,~C3'-endo,BI,canonical,non-pair-contact,helix,stem
   6  C ( A.C2652   0.032  anti,~C3'-endo,BI,canonical,non-pair-contact,helix,stem-end,internal-loop
   7  U . A.U2653   0.019  anti,~C3'-endo,non-canonical,non-pair-contact,helix,internal-loop,phosphate
   8  A . A.A2654   0.019  anti,~C2'-endo,BII,non-canonical,non-pair-contact,helix,internal-loop
   9  G . A.G2655   0.022  turn,anti,~C2'-endo,non-canonical,non-pair-contact,multiplet,internal-loop
  10  U . A.U2656   0.020  anti,~C3'-endo,BI,non-canonical,non-pair-contact,helix,multiplet,internal-loop
      ↪ ,phosphate
  11  A . A.A2657   0.023  anti,~C3'-endo,BI,non-canonical,non-pair-contact,helix,internal-loop
  12  C ( A.C2658   0.013  anti,~C3'-endo,BI,isolated-canonical,non-pair-contact,helix,hairpin-loop,
      ↪ internal-loop
  13  G . A.G2659   0.033  u-turn,anti,~C3'-endo,BI,non-canonical,non-pair-contact,helix-end,hairpin-loop
      ↪ ,cap-acceptor,splayed-apart
  14  U . A.U2660   0.020  turn,u-turn,anti,~C3'-endo,non-pair-contact,hairpin-loop,splayed-apart
  15  A . A.A2661   0.015  u-turn,anti,~C3'-endo,BI,non-pair-contact,hairpin-loop,cap-donor,phosphate
  16  A . A.A2662   0.010  u-turn,anti,~C3'-endo,BI,non-canonical,non-pair-contact,helix-end,hairpin-loop
      ↪ ,phosphate
  17  G ) A.G2663   0.019  anti,~C3'-endo,BI,isolated-canonical,non-pair-contact,helix,hairpin-loop,
      ↪ internal-loop,cap-acceptor
  18  G . A.G2664   0.014  anti,~C3'-endo,BI,non-canonical,non-pair-contact,helix,internal-loop,cap-donor
  19  A . A.A2665   0.014  anti,~C3'-endo,BI,non-canonical,non-pair-contact,helix,multiplet,internal-loop
      ↪ ,phosphate
  20  C . A.C2666   0.016  anti,~C3'-endo,BI,non-canonical,non-pair-contact,helix,internal-loop,phosphate
  21  C . A.C2667   0.029  anti,~C3'-endo,BI,non-canonical,non-pair-contact,helix,internal-loop
  22  G ) A.G2668   0.012  anti,~C3'-endo,BI,canonical,non-pair-contact,helix,stem-end,internal-loop
  23  G ) A.G2669   0.020  anti,~C3'-endo,BI,canonical,non-pair-contact,helix,stem
  24  A ) A.A2670   0.019  anti,~C3'-endo,BI,canonical,non-pair-contact,helix,stem
  25  G ) A.G2671   0.023  anti,~C3'-endo,BI,canonical,non-pair-contact,helix,stem
  26  U ) A.U2672   0.024  anti,~C3'-endo,BI,canonical,non-pair-contact,helix,stem-end
  27  G . A.G2673   0.010  anti,~C3'-endo,non-canonical,non-pair-contact,helix-end,ss-non-loop
```

3.2.13 Backbone torsion angles and suite names

The auto-generated output file named `dssr-torsions.txt` contains many commonly used backbone parameters, including torsion angles, sugar puckers, and suite names[8]. Given below is a summary of the sections contained in the file so that users can better understand what DSSR has to offer.

Main chain conformational parameters Here the single-stranded Zp (ssZp) parameter is an extension to the original 3DNA Zp for distinguishing different types of duplexes[20]. Its addition to 3DNA/DSSR has been inspired by the work of Richardson *et al.*[21], who observed a correlation between the sugar pucker and the perpendicular distance from the 3′-phosphate to the glycosidic bond vector: >2.9 Å for C3′-endo and <2.9 Å for C2′-endo sugars.

Note also the classifications of the backbone into BI/BII forms, χ into *anti*/*syn* conformations, and sugar into C2′-endo/C3′-endo puckers. The collection of relevant information should prove convenient for identification of key backbone features of potential interest.

```
  alpha:   O3'(i-1)-P-O5'-C5'
  beta:    P-O5'-C5'-C4'
  gamma:   O5'-C5'-C4'-C3'
  delta:   C5'-C4'-C3'-O3'
  epsilon: C4'-C3'-O3'-P(i+1)
  zeta:    C3'-O3'-P(i+1)-O5'(i+1)
  e-z:     epsilon-zeta (BI/BII backbone classification)

  chi for pyrimidines(Y): O4'-C1'-N1-C2; purines(R): O4'-C1'-N9-C4
    Range [170, -50(310)] is assigned to anti, and [50, 90] to syn

  phase-angle: the phase angle of pseudorotation and puckering
  sugar-type: ~C2'-endo for C2'-endo like conformation, or
               ~C3'-endo for C3'-endo like conformation
              Note the ONE column offset (for easy visual distinction)

ssZp: single-stranded Zp, defined as the z-coordinate of the 3' phosphorus atom
      (P) expressed in the standard reference frame of the 5' base; the value is
      POSITIVE when P lies on the +z-axis side (base in anti conformation);
      NEGATIVE if P is on the -z-axis side (base in syn conformation)
  Dp: perpendicular distance of the 3' P atom to the glycosidic bond
      [Ref: Chen et al. (2010): "MolProbity: all-atom structure
            validation for macromolecular crystallography."
            Acta Crystallogr D Biol Crystallogr, 66(1):12-21]
splay: angle between the bridging P to the two base-origins of a dinucleotide.
```

There are too many parameters to fit into the page width. The following shows a selected portion of nucleotides in 1msy, with parameters split into two sections.

```
          nt                alpha    beta   gamma   delta  epsilon   zeta     e-z
 5     C A.C2651            -62.3   173.8    46.2    84.3  -154.6   -71.3   -83(BI)
 6     C A.C2652            -67.5   175.2    58.1    78.0  -154.0   -67.0   -87(BI)
```

```
7      U A.U2653          -61.8   167.4    55.9    82.4  -149.4    55.3    155(..)
8      A A.A2654          165.2   133.8    56.7   149.4   -98.3   161.4    100(BII)
9      G A.G2655          -96.2    91.7   179.3   149.3  -167.2   141.4     51(..)
10     U A.U2656          -72.5   157.8    37.9    91.6  -141.0   -65.6    -75(BI)

          nt          chi            phase-angle   sugar-type    ssZp     Dp    splay
5      C A.C2651    -159.0(anti)    12.9(C3'-endo)  ~C3'-endo    4.29    4.58   24.06
6      C A.C2652    -158.8(anti)    15.5(C3'-endo)  ~C3'-endo    4.28    4.53   22.84
7      U A.U2653    -151.0(anti)    15.7(C3'-endo)  ~C3'-endo    4.00    4.62   22.57
8      A A.A2654    -145.3(anti)   151.0(C2'-endo) ~C2'-endo     0.91    0.92   43.08
9      G A.G2655     -93.5(anti)   151.5(C2'-endo) ~C2'-endo     2.15    2.14   54.21
10     U A.U2656    -173.9(anti)     0.4(C3'-endo)  ~C3'-endo    4.35    4.42   27.39
```

Virtual torsion angles Three sets of virtual torsion angles are calculated: one is the most commonly used η/θ pair pioneered by Olson[22]; the second is its η'/θ' variant (using the C1′ atom instead of C4′) later introduced by Pyle *et al.*[23]; and the third (termed η''/θ'') takes advantage of the origin of the base reference frame[4] in place of the C4′ or C1′ atom. The set of base-phosphorus virtual torsions is unique to 3DNA/DSSR.

```
 eta:    C4'(i-1)-P(i)-C4'(i)-P(i+1)
 theta:  P(i)-C4'(i)-P(i+1)-C4'(i+1)
   [Ref: Olson (1980): "Configurational statistics of polynucleotide chains.
         An updated virtual bond model to treat effects of base stacking."
         Macromolecules, 13(3):721-728]

 eta':   C1'(i-1)-P(i)-C1'(i)-P(i+1)
 theta': P(i)-C1'(i)-P(i+1)-C1'(i+1)
   [Ref: Keating et al. (2011): "A new way to see RNA." Quarterly Reviews
         of Biophysics, 44(4):433-466]

 eta":   base(i-1)-P(i)-base(i)-P(i+1)
 theta": P(i)-base(i)-P(i+1)-base(i+1)

          nt                 eta   theta     eta'  theta'    eta"  theta"
1      U A.U2647              ---     ---     ---     ---     ---     ---
2      G A.G2648            172.1  -133.3  -163.5  -131.2   -97.6   -93.1
3      C A.C2649            162.7  -140.1  -178.0  -138.9  -120.5  -104.8
4      U A.U2650            167.0  -148.3  -174.5  -150.1  -122.6  -127.9
5      C A.C2651            165.4  -147.2   177.6  -145.6  -144.3  -123.9
6      C A.C2652            171.3  -142.0  -176.3  -139.3  -142.0   -91.5
7      U A.U2653            172.2   -18.3  -170.0   -63.3  -107.9   -99.1
8      A A.A2654             46.3   172.0   120.5   135.6   126.4   150.3
9      G A.G2655            -44.2    24.9   -82.3    59.0   -98.6    91.3
10     U A.U2656            170.9  -121.7   163.1  -122.7   161.9   -94.8
11     A A.A2657            162.1  -127.4  -177.7  -123.2  -126.9   -67.0
12     C A.C2658            159.4  -135.3  -176.0  -135.4   -98.2  -106.5
13     G A.G2659            167.6  -117.7  -179.4  -160.6  -134.1   156.9
14     U A.U2660             15.1  -126.1    43.5  -124.9    21.0   -65.2
15     A A.A2661            160.4  -132.0  -169.4  -138.7   -95.8   -93.3
16     A A.A2662            167.0   -83.0  -174.8   -81.7  -117.0   -64.2
17     G A.G2663            172.6  -154.0  -148.2  -148.6  -101.2   -97.0
18     G A.G2664            166.2   166.9  -168.9   147.4   -95.5   137.9
19     A A.A2665           -155.6   141.6   175.0   164.3   154.7  -178.6
20     C A.C2666           -178.4  -125.3  -169.0  -123.0  -153.9   -74.8
21     C A.C2667            164.6  -120.7  -172.9  -116.0  -101.6   -71.6
22     G A.G2668            164.9  -150.0  -168.4  -145.8   -97.4  -120.2
```

```
 23     G A.G2669            171.3  -139.8  -172.8  -139.5  -131.7  -111.7
 24     A A.A2670            170.6  -153.2  -173.8  -152.7  -127.2  -132.0
 25     G A.G2671            170.4  -134.4  -180.0  -133.1  -147.1   -94.7
 26     U A.U2672            172.2  -167.9  -166.6  -170.6  -110.6  -171.6
 27     G A.G2673              ---     ---     ---     ---     ---     ---
```

Sugar conformational parameters By default, the sugar pucker analysis follows the work of Altona and Sundaralingam[24]. The phase angle (in the range of 0° to 360°) of pseudorotation is divided equally into ten 36° regions; the two most frequent sugar pucker modes are the C3′-endo [0°, 36°) as in canonical RNA and A-form DNA, and the C2′-endo [144°, 180°) as in standard B-form DNA. Where appropriate, each sugar pucker is assigned into either ∼C3′-endo or ∼C2′-endo (see above in Section 3.2.13 under 'sugar-type') by matching against corresponding fiber models.

```
  v0: C4'-O4'-C1'-C2'
  v1: O4'-C1'-C2'-C3'
  v2: C1'-C2'-C3'-C4'
  v3: C2'-C3'-C4'-O4'
  v4: C3'-C4'-O4'-C1'

  tm: the amplitude of pucker
  P:  the phase angle of pseudorotation
    [Ref: Altona & Sundaralingam (1972): "Conformational analysis
          of the sugar ring in nucleosides and nucleotides. A new
          description using the concept of pseudorotation."
          J Am Chem Soc, 94(23):8205-8212]

          nt                 v0      v1      v2      v3      v4      tm      P   Puckering
1     U A.U2647              7.5   -34.5    46.2   -43.8    23.1    46.9    9.9  C3'-endo
2     G A.G2648              9.5   -31.5    39.4   -35.5    16.8    39.6    5.3  C3'-endo
3     C A.C2649              4.0   -28.3    39.9   -38.4    21.9    40.9   12.9  C3'-endo
4     U A.U2650             -2.4   -25.5    41.9   -44.0    29.4    44.9   21.3  C3'-endo
5     C A.C2651              4.8   -32.5    45.7   -44.6    25.0    46.9   12.9  C3'-endo
6     C A.C2652              2.9   -29.7    43.8   -44.0    25.9    45.4   15.5  C3'-endo
7     U A.U2653              1.6   -28.2    42.3   -41.3    25.2    44.0   15.7  C3'-endo
8     A A.A2654            -33.2    44.3   -38.7    20.1     8.5    44.3  151.0  C2'-endo
9     G A.G2655            -37.3    50.1   -43.9    22.9     8.9    50.0  151.5  C2'-endo
10    U A.U2656             12.7   -32.9    39.6   -33.2    13.3    39.6    0.4  C3'-endo
11    A A.A2657             -6.4   -21.7    39.9   -44.5    32.0    44.6   26.5  C3'-endo
12    C A.C2658             -0.0   -28.5    44.6   -44.4    28.4    46.9   17.9  C3'-endo
13    G A.G2659             -9.4   -20.6    40.1   -45.3    35.5    46.1   29.4  C3'-endo
14    U A.U2660             -8.9   -14.6    31.3   -37.4    29.0    37.0   32.3  C3'-endo
15    A A.A2661              7.2   -28.7    38.3   -35.0    17.5    38.6    8.0  C3'-endo
16    A A.A2662              0.0   -21.1    32.9   -33.9    21.4    34.8   18.7  C3'-endo
17    G A.G2663             -7.9   -22.7    42.3   -47.3    35.7    47.8   27.7  C3'-endo
18    G A.G2664              7.4   -33.6    45.9   -43.1    22.1    46.5    9.7  C3'-endo
19    A A.A2665             11.2   -35.6    45.2   -39.6    18.1    45.4    4.5  C3'-endo
20    C A.C2666              2.0   -27.6    41.2   -41.2    24.6    42.8   16.0  C3'-endo
21    C A.C2667              1.9   -30.7    45.7   -46.0    28.2    47.6   16.5  C3'-endo
22    G A.G2668              9.1   -34.4    44.4   -40.9    20.0    44.7    7.3  C3'-endo
23    G A.G2669              4.5   -31.3    45.1   -43.5    24.4    46.3   13.0  C3'-endo
24    A A.A2670              5.3   -32.9    46.7   -45.3    25.1    47.9   12.6  C3'-endo
25    G A.G2671              7.6   -33.2    44.6   -41.4    21.7    45.2    9.2  C3'-endo
26    U A.U2672             -0.3   -23.0    35.9   -37.6    23.6    38.0   19.2  C3'-endo
```

```
 27    G A.G2673            17.1    -39.6    45.4    -37.1    12.9    45.4    357.2    C2'-exo
```

Assignment of sugar-phosphate backbone suite names According to Richardson *et al.*[8], the backbone suite is defined as the sugar-to-sugar version of a nucleotide (in contrast to the traditional definition as a phosphate-to-phosphate unit). A total of 53 backbone conformer bins have been defined and expressed in mnemonic 2-letter names (e.g., `1a`, `5z`, with outliers signified by `!!`).

```
  bin: name of the 12 bins based on [delta(i-1), delta, gamma], where
       delta(i-1) and delta can be either 3 (for C3'-endo sugar) or 2
       (for C2'-endo) and gamma can be p/t/m (for gauche+/trans/gauche-
       conformations, respectively) (2x2x3=12 combinations: 33p, 33t,
       ... 22m); 'inc' refers to incomplete cases (i.e., with missing
       torsions), and 'trig' to triages (i.e., with torsion angle
       outliers)
  cluster: 2-char suite name, for one of 53 reported clusters (46
           certain and 7 wannabes), '__' for incomplete cases, and
           '!!' for outliers
  suiteness: measure of conformer-match quality (low to high in range 0 to 1)

    [Ref: Richardson et al. (2008): "RNA backbone: consensus all-angle
          conformers and modular string nomenclature (an RNA Ontology
          Consortium contribution)." RNA, 14(3):465-481]

          nt              bin     cluster   suiteness
 1     U A.U2647          inc       __        0
 2     G A.G2648          33p       1a        0.052
 3     C A.C2649          33p       1a        0.665
 4     U A.U2650          33p       1a        0.875
 5     C A.C2651          33p       1a        0.871
 6     C A.C2652          33p       1a        0.919
 7     U A.U2653          33p       1a        0.929
 8     A A.A2654          32p       5z        0.849
 9     G A.G2655          22t       4s        0.730
 10    U A.U2656          23p       #a        0.842
 11    A A.A2657          33p       1a        0.693
 12    C A.C2658          33p       1a        0.884
 13    G A.G2659          33p       1a        0.894
 14    U A.U2660          33p       1g        0.736
 15    A A.A2661          33p       1L        0.688
 16    A A.A2662          33p       1a        0.692
 17    G A.G2663          33t       1c        0.321
 18    G A.G2664          33p       1a        0.878
 19    A A.A2665          33t       1e        0.875
 20    C A.C2666          33p       1a        0.891
 21    C A.C2667          33p       1a        0.887
 22    G A.G2668          33p       1a        0.756
 23    G A.G2669          33p       1a        0.625
 24    A A.A2670          33p       1a        0.914
 25    G A.G2671          33p       1a        0.878
 26    U A.U2672          33p       1a        0.912
 27    G A.G2673          trig      !!        0

Concatenated suite string per chain. To avoid confusion of lower case
modified nucleotide name (e.g., 'a') with suite cluster (e.g., '1a'),
use --suite-delimiter to add delimiters (matched '()' by default).
```

```
1   A RNA nts=27  U1aG1aC1aU1aC1aC1aU5zA4sG#
    ↪ aU1aA1aC1aG1gU1LA1aA1cG1aG1eA1aC1aC1aG1aG1aA1aG1aU!!G
```

Note that in assigning suite names, the χ torsion angle, which characterizes the relative sugar-base orientation, is not taken into consideration. Moreover, the 53 defined backbone conformer bins are RNA-centric: even for the classic B-DNA Dickerson dodecamer (355d), 16 out of 22 suites (∼73%) are classified as outliers (`!!`).

3.3 Default run on PDB entry 1ehz (tRNA^{Phe}): summary notes

The cloverleaf 2D structure of tRNA has become an iconic image in structural biology. The four stems (the acceptor stem, the D stem, the anti-codon stem, and the T stem) form two halves of the L-shaped tertiary structure through coaxial stacking of two pairs of stems. Yet, other than DSSR, there appear to be no alternative software programs that can neatly delineate the L-shaped 3D vs. the cloverleaf 2D structures of a tRNA molecule from atomic coordinates. The cover image of the manual illustrates DSSR's capability to solve this long-standing problem, using 1ehz, the crystal structure of yeast phenylalanine tRNA, as an example.

3.3.1 Brief summary

The screen output of a DSSR run on 1ehz (assuming the 3D coordinates file is called `1ehz.pdb`) is shown below. Note that DSSR correctly identifies two helices, four stems, three hairpin loops, and one four-way junction loop, among other things.

```
    total number of nucleotides: 76
           modified nucleotides: 14
    total number of base pairs: 34
    total number of helices: 2
    total number of stems: 4
    total number of isolated WC/wobble pairs: 1
    total number of multiplets: 4
    total number of atom-base capping interactions: 4
    total number of splayed-apart dinucleotides: 9
                        consolidated into units: 6
    total number of hairpin loops: 3
    total number of junctions: 1
    total number of non-loop single-stranded segments: 1
    total number of kissing loops: 1

Time used: 00:00:00:00
```

3.3.2 Modified nucleotides

The 27-nt long RNA fragment 1msy detailed in Section 3.2 contains only canonical nts (A, C, G, and U). However, 14 out of the 76 nts in $tRNA^{Phe}$ 1ehz are modified (of 11 different types), as listed below.

```
List of 11 types of 14 modified nucleotides
      nt     count  list
   1 1MA-a     1    A.1MA58
   2 2MG-g     1    A.2MG10
   3 5MC-c     2    A.5MC40,A.5MC49
   4 5MU-t     1    A.5MU54
   5 7MG-g     1    A.7MG46
   6 H2U-u     2    A.H2U16,A.H2U17
   7 M2G-g     1    A.M2G26
   8 OMC-c     1    A.OMC32
   9 OMG-g     1    A.OMG34
  10 PSU-P     2    A.PSU39,A.PSU55
  11 YYG-g     1    A.YYG37
```

Details about each of the 11 types of modified nts are: a 3-letter residue name followed by its 1-letter shorthand form (under column `nt`), its frequency (under column `count`), and a comma separated enumeration of its occurrences (under column `list`). For example, 5MC (no. 3) is found twice in 1ehz, with residue numbers 40 and 49, respectively.

From its 3-letter residue name, further information about a modified nt can be obtained via RCSB Ligand Explorer. For example, click the link to check `H2U` (5,6-dihydrouridine-5'-monophosphate).

3.3.3 The four triplets

DSSR detects four base triplets as listed below. Use Jmol/PyMOL to visualize the output file `dssr-multiplets.pdb` for verification.

```
List of 4 multiplets
   1 nts=3 UAA A.U8,A.A14,A.A21
   2 nts=3 AUA A.A9,A.U12,A.A23
   3 nts=3 gCG A.2MG10,A.C25,A.G45
   4 nts=3 CGg A.C13,A.G22,A.7MG46
```

3.3.4 Relationship between helices and stems

The connection between the two helices and the four stems is available from the main output file, with related portions excerpted below. The meaning of each section should be

easy to follow, especially in connection with the tRNA^{Phe} (1ehz) 2D structure image shown on the cover of this manual.

```
  helix#1[2] bps=15
  helix#2[2] bps=15

  stem#1[#1] bps=7
  stem#2[#2] bps=4
  stem#3[#2] bps=4
  stem#4[#1] bps=5

List of 2 coaxial stacks
   1 Helix#1 contains 2 stems: [#1,#4]
   2 Helix#2 contains 2 stems: [#3,#2]
```

3.3.5 Three hairpin loops

As expected, three hairpin loops are identified, with details listed below.

```
List of 3 hairpin loops
   1 hairpin loop: nts=10; [8]; linked by [#2]
     summary: [1] 8 [A.13 A.22] 4
     nts=10 CAGuuGGGAG A.C13,A.A14,A.G15,A.H2U16,A.H2U17,A.G18,A.G19,A.G20,A.A21,A.G22
       nts=8 AGuuGGGA A.A14,A.G15,A.H2U16,A.H2U17,A.G18,A.G19,A.G20,A.A21
   2 hairpin loop: nts=11; [9]; linked by [#3]
     summary: [1] 9 [A.30 A.40] 4
     nts=11 GAcUgAAgAPc A.G30,A.A31,A.OMC32,A.U33,A.OMG34,A.A35,A.A36,A.YYG37,A.A38,A.PSU39,
         ↪ A.5MC40
       nts=9 AcUgAAgAP A.A31,A.OMC32,A.U33,A.OMG34,A.A35,A.A36,A.YYG37,A.A38,A.PSU39
   3 hairpin loop: nts=9; [7]; linked by [#4]
     summary: [1] 7 [A.53 A.61] 5
     nts=9 GtPCGaUCC A.G53,A.5MU54,A.PSU55,A.C56,A.G57,A.1MA58,A.U59,A.C60,A.C61
       nts=7 tPCGaUC A.5MU54,A.PSU55,A.C56,A.G57,A.1MA58,A.U59,A.C60
```

3.3.6 One four-way junction loop

The four-way junction loop is delineated by the four stems (`[#1,#2,#3,#4]`), with `[2,1,5,0]` nucleotides connecting each consecutive stems. This loop is well-documented in literature, forming the core of the cloverleaf: see the cover image on the right, and also the 2015 DSSR paper[1]. Note that the junction loop contains four modified nucleotides (2MG10, M2G26, 7MG46, 5MC49), which pose a problem for some RNA structural analysis programs.

```
List of 1 junction
   1 4-way junction: nts=16; [2,1,5,0]; linked by [#1,#2,#3,#4]
     summary: [4] 2 1 5 0 [A.7 A.66 A.10 A.25 A.27 A.43 A.49 A.65] 7 4 4 5
     nts=16 UUAgCgCGAGgUCcGA A.U7,A.U8,A.A9,A.2MG10,A.C25,A.M2G26,A.C27,A.G43,A.A44,A.G45,A
         ↪ .7MG46,A.U47,A.C48,A.5MC49,A.G65,A.A66
       nts=2 UA A.U8,A.A9
```

```
      nts=1 g A.M2G26
      nts=5 AGgUC A.A44,A.G45,A.7MG46,A.U47,A.C48
      nts=0
```

3.3.7 Pseudoknot

The tRNA^{Phe} 1ehz contains a pseudoknot, due to the formation of the canonical G–C pair between G19 and C56 (see the long cyan line in the 2D representation on the cover image). This pair is conserved and located at the elbow of the L-shaped tertiary structure that brings the D-loop and the TΨC-loop together, via essentially a simple kissing loop interaction. The elbow G–C pair has been shown to stack against a base triplet of the T-box riboswitch[25], apparently playing an import role in forming the stem-I-tRNA complex (`4lck`).

In DSSR dbn output, the bps in first-order pseudoknots are designated by matched square brackets, as shown below for 1ehz.

```
>1ehz-A #1 nts=76 0.09(2.86) [chain] RNA
GCGGAUUUAgCUCAGuuGGGAGAGCgCCAGAcUgAAgAPcUGGAGgUCcUGUGtPCGaUCCACAGAAUUCGCACCA
(((((((..((((.....[..)))).((((.........)))).....((((..].....)))))))))))).....
```

For bps in higher-order pseudoknots, matched curly brackets `{}`, angle brackets `<>`, or upper-lower case letters (`Aa`, `Bb`, `Cc` etc.) are used. Please refer to Section 3.6 for an example.

3.4 Default run on PDB entry 1jj2: four auto-checked motifs

The crystal structure of the *Haloarcula marismortui* large ribosomal subunit (1jj2) serves as an example on how DSSR can analyze complicated RNA structures as easily as smaller ones (such as 1msy and 1ehz discussed in previous sections). Let the PDB 3D atomic coordinates file be called `1jj2.pdb`, the screen output is shown below. The running time will obviously depend on hardware configurations.

```
    total number of nucleotides: 2876
    total number of amino acids: 3701
    total number of base pairs: 1474
    total number of helices: 87
    total number of stems: 179
    total number of isolated WC/wobble pairs: 53
    total number of multiplets: 252
    total number of atom-base capping interactions: 239
    total number of splayed-apart dinucleotides: 409
                        consolidated into units: 257
    total number of hairpin loops: 68
    total number of bulges: 39
    total number of internal loops: 66
```

```
    total number of junctions: 37
    total number of non-loop single-stranded segments: 30
    total number of kissing loops: 5
    total number of A-minor (types I and II) motifs: 107
    total number of eXtended A-minor (type X) motifs: 49
    total number of ribose zippers: 46
    total number of kink turns: 8

Time used: 00:00:00:37
```

Notice the large numbers of bps, multiplets, loops (of various types), and four additional motifs—kissing loops, A-minor motifs, ribose zippers, and k-turns—that will be discussed in detail in the following sections.

As a side note, DSSR detects an additional base pentaplet (`AUAAG`, see Figure 10) which was missed using 3DNA[9]. The five nts (`A306`, `U325`, `A331`, `A340`, and `G345`), all on chain 0, form five base-base H-bonds as well as four additional H-bonding interactions involving O2′ atoms. Overall, in default settings, DSSR is more sophisticated than the 3DNA `find_pair` program in identifying bps, multiplets, and double helical regions.

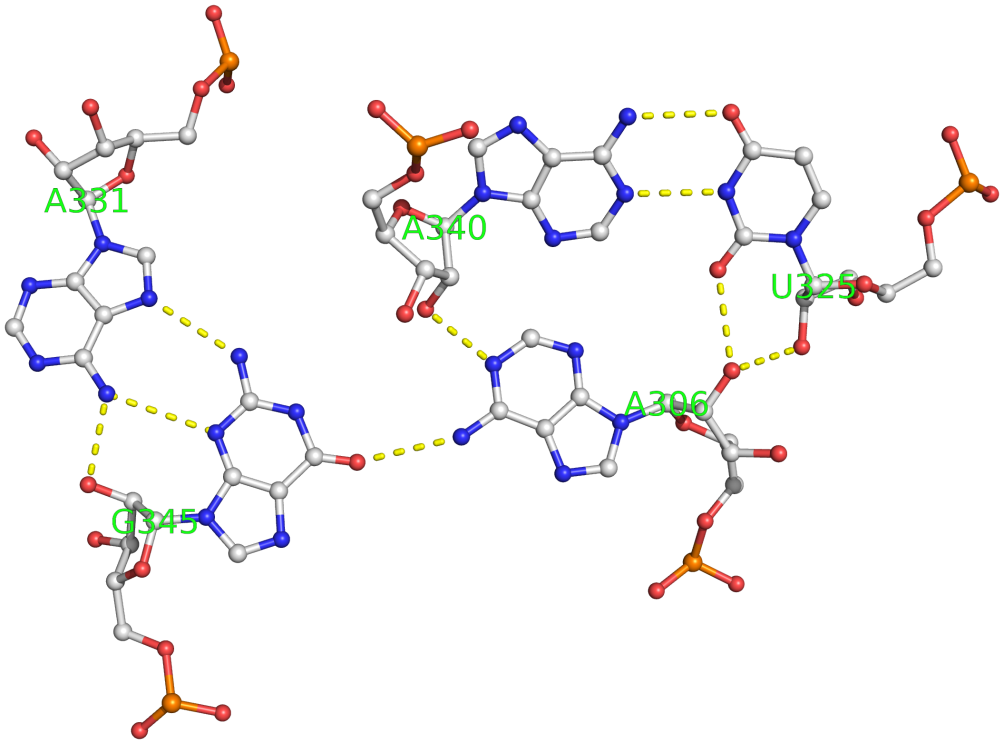

Figure 10: The additional base pentaplet (`AUAAG`) identified by DSSR but missed using 3DNA[9]. Here all five nts are derived from chain 0 of 1jj2. The image was produced with PyMOL.

3.4.1 Kissing loops

The kissing-loop motif is characterized by canonical base-pairing interactions (forming a stem) between two hairpin loops. Five such motifs are identified in 1jj2 as listed below, and no. 5 is illustrated in Figure 11.

```
List of 5 kissing loop interactions
   1 isolated-pair #-42 between hairpin loops #51 and #53
   2 isolated-pair #-6 between hairpin loops #6 and #8
   3 stem #8 between hairpin loops #1 and #3
   4 stem #9 between hairpin loops #1 and #3
   5 stem #29 between hairpin loops #14 and #57
```

The stem (#29) referred to above is:

```
  stem#29[#15] bps=6
      strand-1 5'-CAUCGA-3'
       bp-type    ||||||
      strand-2 3'-GUAGUU-5'
      helix-form  AAA..
   1 0.C418         0.G2449        C-G WC           19-XIX     cWW  cW-W
   2 0.A419         0.U2448        A-U WC           20-XX      cWW  cW-W
   3 0.U420         0.A2447        U-A WC           20-XX      cWW  cW-W
   4 0.C421         0.G2446        C-G WC           19-XIX     cWW  cW-W
   5 0.G422         0.U2445        G-U Wobble       28-XXVIII cWW  cW-W
   6 0.A423         0.U2444        A-U WC           20-XX      cWW  cW-W
```

The two interacting hairpin loops (#14 and #57) are:

```
  14 hairpin loop: nts=9; [7]; linked by [#28]
     summary: [1] 7 [0.416 0.424] 5
     nts=9 GGCAUCGAC 0.G416,0.G417,0.C418,0.A419,0.U420,0.C421,0.G422,0.A423,0.C424
       nts=7 GCAUCGA 0.G417,0.C418,0.A419,0.U420,0.C421,0.G422,0.A423

  57 hairpin loop: nts=9; [7]; linked by [#145]
     summary: [1] 7 [0.2442 0.2450] 5
     nts=9 GCUUGAUGC 0.G2442,0.C2443,0.U2444,0.U2445,0.G2446,0.A2447,0.U2448,0.G2449,0.C2450
       nts=7 CUUGAUG 0.C2443,0.U2444,0.U2445,0.G2446,0.A2447,0.U2448,0.G2449
```

3.4.2 A-minor motifs

The interaction of the minor groove edge of an adenine with the minor groove side of a canonical pair is defined as the A-minor motif[16]. This abundant structural motif stabilizes RNA tertiary structures. Depending on the position of the adenine with respect to the interacting pair, the A-minor motif has been further divided into four subtypes. Of these, only two types (I and II) are believed to be adenine-specific, and they are identified by DSSR (see Figure 12).

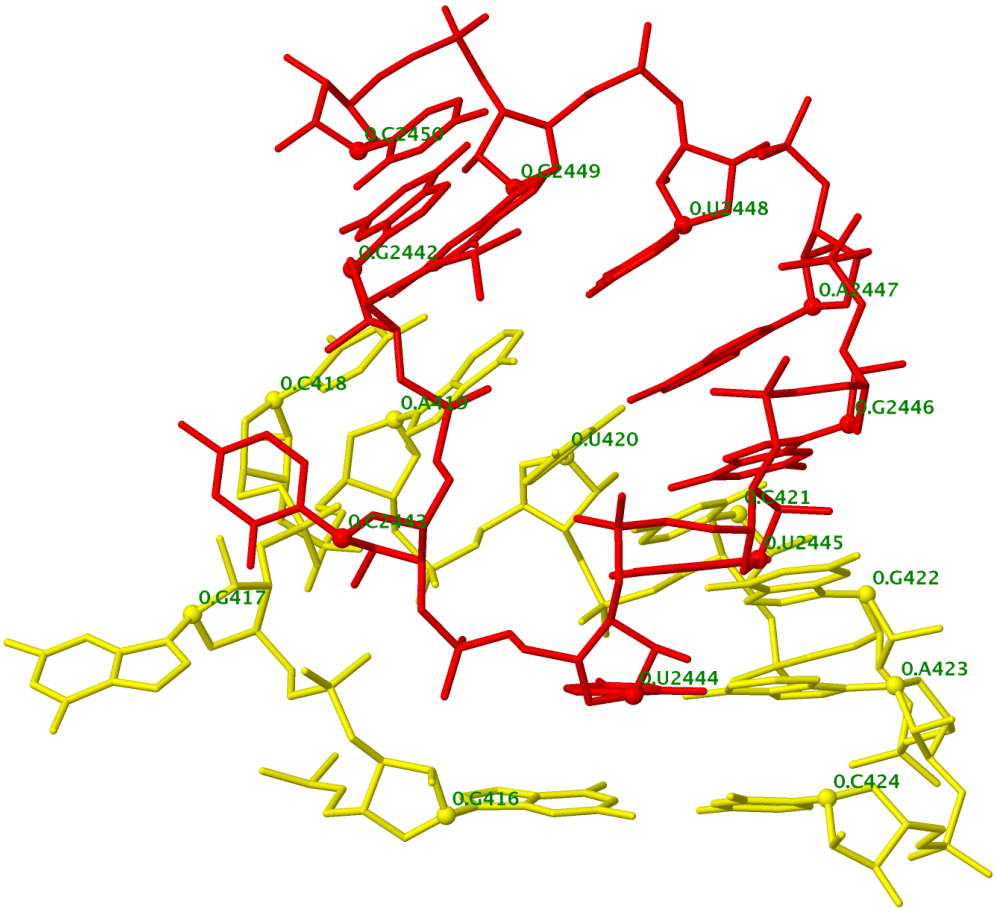

Figure 11: One kissing-loop motif identified in 1jj2. Here, one hairpin loop is colored yellow (#14, with nts from 416 to 424 on chain 0), and the other red (#57, with nts from 2442 to 2450 on the same chain). Six base pairs formed between the two loop regions constitute stem #29. The image was produced with Jmol.

A new type, designated X (eXtended, for cases other than the classic types I and II), was also identified by DSSR. In types I and II A-minor motifs, the adenine has its minor groove edge facing the minor groove of a canonical pair, and the O2′ atom of adenine is involved in H-bonding interactions with the pair. In the miscellaneous type X, the adenine uses its Watson-Crick edge or major-groove edge to interact with the minor groove of a canonical pair, without resorting to the O2′ atom. This type of A-minor interactions was reported in the crystal structure of the self-cleaving Pistol ribozyme[26].

DSSR is unique in using standard base reference frames (Figure 1B) and bp parameters to characterize A-minor motifs. When applied to 1jj2, a total of 156 A-minor motifs were

identified (stored in file `dssr-Aminors.pdb`), including type X cases. Three sample entries, each for types I, II, and X, are listed below: no. 4 for type I, no. 7 for type II (see also Figure 12), and no. 11 for type X.

```
List of 156 A-minor motifs (types I, II, or X)
   4  type=I A|G-C      0.A69|0.G54,0.C65 WC
        +0.G54  H-bonds[2]: "N1-O2'(hydroxyl)[2.69],N3-N2(amino)[2.84]"
        -0.C65  H-bonds[2]: "O2'(hydroxyl)-O2'(hydroxyl)[2.62],O2'(hydroxyl)-O2(carbonyl)
            ↪ [2.61]"

   7  type=II A|G-C     0.A152|0.G41,0.C440 WC
        +0.G41  H-bonds[0]: ""
        -0.C440 H-bonds[3]: "O2'(hydroxyl)-O3'[3.17],O2'(hydroxyl)-O2'(hydroxyl)[2.73],N3-O2
            ↪ '(hydroxyl)[2.70]"

  11  type=X A|U-G      0.A166|0.U919,0.G924 Wobble
        -0.U919 H-bonds[0]: ""
        +0.G924 H-bonds[3]: "N6(amino)-O2'(hydroxyl)[2.90],N6(amino)-N3[3.15],N1-N2(amino)
            ↪ [2.98]"
```

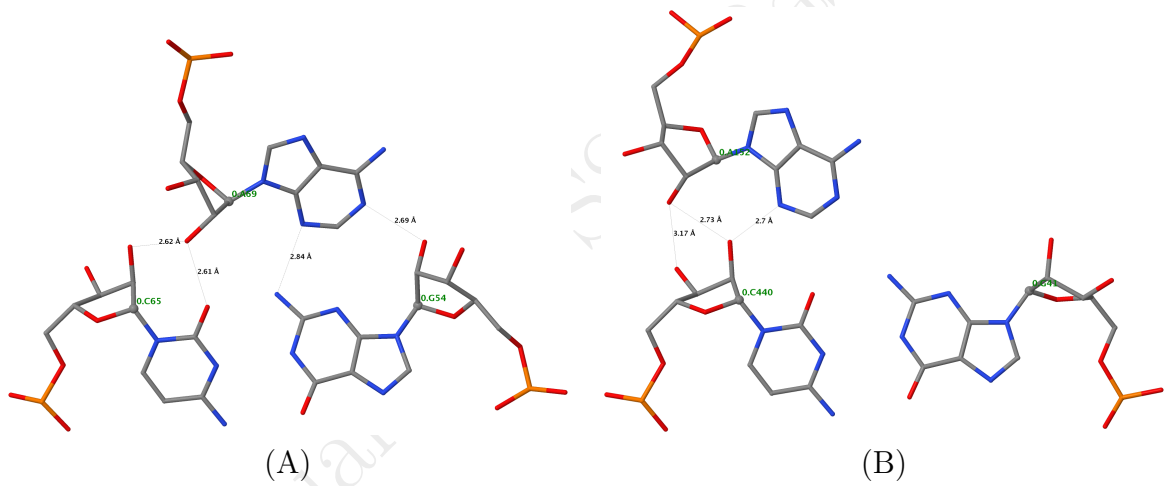

Figure 12: Two types of A-minor motifs presumably to be specific to adenine. (A) Type I, where the O2′ and N3 atoms of adenine lie inside the minor-groove edge of the canonical base pair; (B) Type II, where the O2′ of adenine lies outside but N3 remains inside the minor-groove edge. The images were produced with Jmol.

For each entry, the type (I, II, or X) is followed by the A-minor motif identity first in one-letter shorthand notation (e.g., `A|G-C`) and then the corresponding full specification of the interacting nts (e.g., `0.A69|0.G54,0.C65`). The canonical bp name (WC or wobble) is added at the end. The following two lines list the relative orientation (+ or −)[9] and the H-bonding interactions that each nt of the canonical pairs has with adenine, respectively. Thus for the

type I A-minor motif no. 4 listed above, `+0.G54` means that `0.G54` and `0.A69` have similar faces (i.e., the dot product of the z-axes of their base reference frames is positive). Conversely, `0.A69` and `0.C65` have opposite faces, so `-0.C65` is placed in the next line.

As one can see from the above listing, in type I A-minor motifs the adenine interacts with both nucleotides of the pair. In type II or X, on the other hand, the adenine interacts with only one of paired nucleotides.

3.4.3 Ribose zippers

First described in the P4-P6 domain of a group I intron[27], the ribose zipper is a tertiary interaction that is important for RNA packing. In DSSR, a ribose-zipper motif is defined by two or more (very rare) consecutive H-bonds between ribose 2′-hydroxyl groups from two RNA fragments (see Figure 13).

In 1jj2, DSSR detects a total of 46 ribose zippers, all consisting of 2×2 nts. The first twelve zippers are listed below, and the top one is illustrated in Figure 13.

```
List of 46 ribose zippers
   1 nts=4 UUAG 0.U26,0.U27,0.A1318,0.G1319
   2 nts=4 ACAC 0.A152,0.C153,0.A439,0.C440
   3 nts=4 AACC 0.A160,0.A161,0.C769,0.C770
   4 nts=4 AGAU 0.A189,0.G190,0.A204,0.U205
   5 nts=4 CGAA 0.C208,0.G209,0.A665,0.A666
   6 nts=4 UAAA 0.U233,0.A234,0.A436,0.A437
   7 nts=4 AACC 0.A242,0.A243,0.C376,0.C377
   8 nts=4 AAUG 0.A305,0.A306,0.U325,0.G326
   9 nts=4 GAAC 0.G471,0.A472,0.A773,0.C774
  10 nts=4 AACC 0.A520,0.A521,0.C637,0.C638
  11 nts=4 AACC 0.A551,0.A552,0.C1334,0.C1335
  12 nts=4 AACU 0.A565,0.A566,0.C1263,0.U1264
  . . . . . . . . . . . . . . . . . . . . . .
```

3.4.4 Kink turns

The kink-turn (k-turn), first characterized in the large ribosomal subunit of *H. marismortui*[28], is a widespread structural motif in RNA. The motif contains a sharp kink in the RNA helix, with an asymmetric internal loop flanked by C–G bps on one side and sheared G–A bps on the other. The Lilley laboratory established a systematic nomenclature for nucleotides[29] and maintains a dedicated database for k-turns.

By default, DSSR defines a k-turn motif as an asymmetric internal loop with at least one sheared G–A pair and a large bending angle in the helical axis, among other criteria. The program detects three types of k-turns: normal, reverse, or else (for possible but undecided

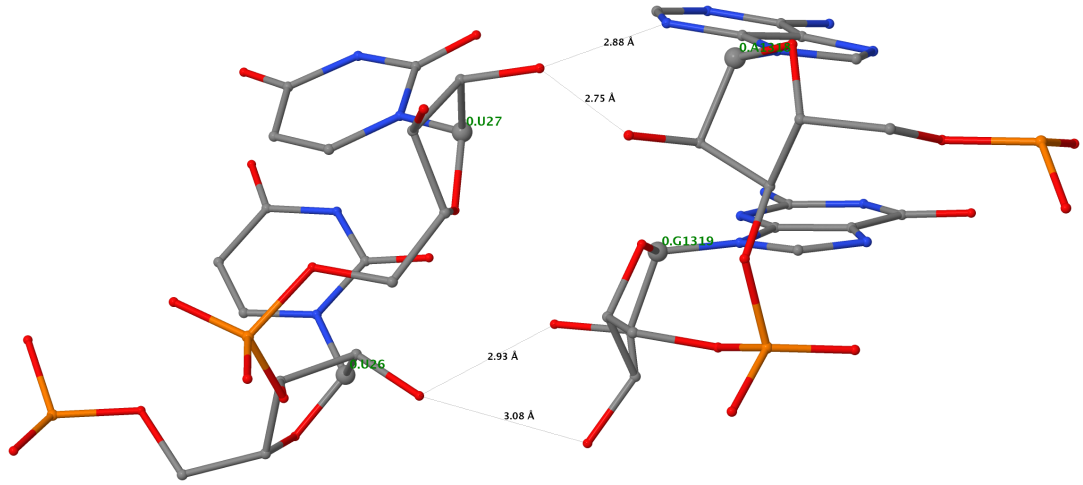

Figure 13: A sample canonical ribose zipper identified in 1jj2. This motif consists of the `U26-U27` dinucleotide in one strand, and `A1318-G1319` in the other, both on chain 0. The images were produced with Jmol.

cases). The normal type includes simple (standard or non-standard) and complex k-turns as defined by Lilley[30], as long as they involve asymmetric internal loops. DSSR finds a total of eight k-turns in 1jj2, the first of which (commonly known as *H. marismortui* Kt-7) is listed below and depicted in Figure 14.

```
1 Normal k-turn; iloop#43; between stems [#11,#10]; bending-angle=54
  C#11[CG 0.C93,0.G81] [GA 0.G97,0.A80] NC#10[CG 0.C100,0.G77]
  strand1 nts=15; GGCGAAGAACCAUGG 0.G91,0.G92,0.C93,0.G94,0.A95,0.A96,0.G97,0.A98,0.A99
      ↪ ,0.C100,0.C101,0.A102,0.U103,0.G104,0.G105
  strand2 nts=12; CCAUGGGGAGCC 0.C72,0.C73,0.A74,0.U75,0.G76,0.G77,0.G78,0.G79,0.A80,0.
      ↪ G81,0.C82,0.C83
```

- The 1st line means that this is a normal k-turn, derived from internal loop `#43` (which is delineated by stems `#11` and `#10`). The bending angle between the two stems is 54°.
- The 2nd line shows that the canonical helix consists of stem `#11`, with a C–G pair (`0.C93` and `0.G81`) closing the internal loop at one end. The non-canonical helix contains stem `#10`, with a C–G pair (`0.C100` and `0.G77`) closing the internal loop at the other end. The crucial sheared G–A pair is formed by `0.G97` and `0.A80` (highlighted with thick lines in Figure 14). See reference[29] for nomenclature of C and NC helices in k-turns.
- The 3rd and 4th lines list the two strands composing the k-turn.

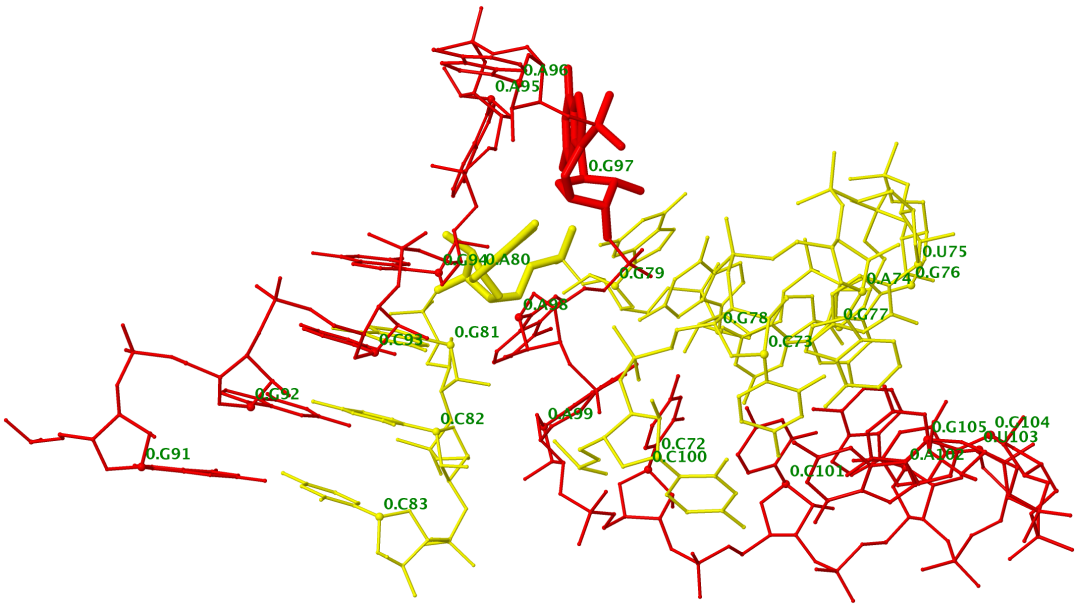

Figure 14: A normal k-turn identified in 1jj2, commonly known as *H. marismortui* Kt-7. The two strands are colored yellow and red, respectively, for easy visualization of the backbone trajectory. The crucial sheared G–A pair is highlighted with thick lines. The image was produced with Jmol.

3.5 Identification and characterization of G-quadruplexes

G-quadruplexes (hereafter referred to as G4) are a common type of higher-order DNA and RNA structures formed from G-rich sequences[31–33]. The building block of G4 is a tetrad of guanines in a cyclic 'planar' alignment, with four G+G pairs (cW+M type, see Figure 15). A G4 is formed by stacking of G-tetrads and stabilized by cations. G4 structures are polymorphic: the four strands can be parallel or anti-parallel, and loops connecting them can be of different types: lateral (edgewise), diagonal, or propeller (double-chain reversal). Moreover, G4 structures can be intra- or intermolecular, and even contain bulges[34]. Overall, G4 can take a large variety of topologies.

DSSR has a dedicated module that streamlines the analysis, annotations, and visualization of G4 structures. See Figures 15 and 16, and http://g4.x3dna.org/ (DSSR-G4DB: G-quadruplexes auto-curated with DSSR from the PDB).

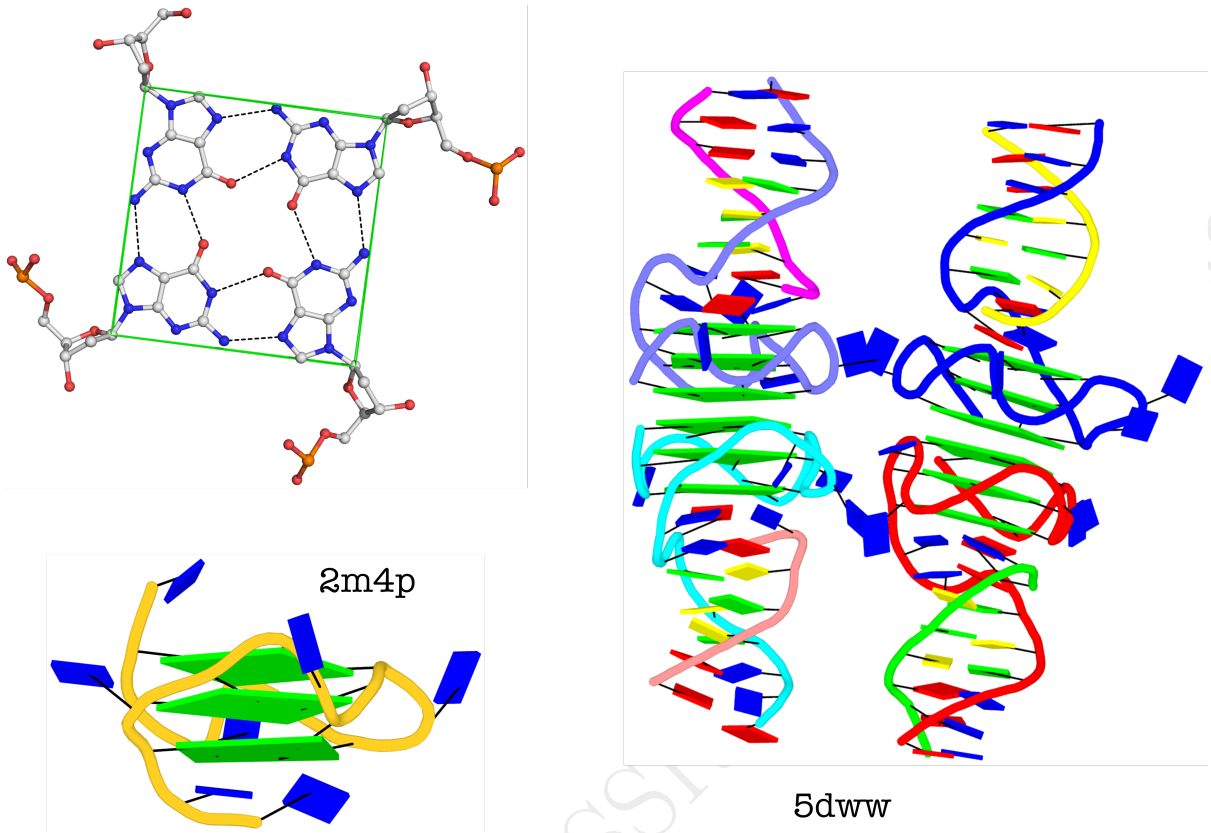

Figure 15: Representative G4 structures. Upper left: atomic structure of G-tetrad, the building block of G4 structures. Here the green 'square' is created by connecting the C1′ atoms of the guanosines, and it is used to simplify the representation of G4 structures of PDB entries 2m4p (lower left) and 5dww (right). Note that the asymmetric unit of 5dww contains four biological units, which are coaxially stacked into two columns.

3.6 Pseudoknots detection and removal

RNA pseudoknot is defined by WC pairing interactions between bases in a hairpin loop and those outside the corresponding stem. Intuitively, WC pairs in pseudoknotted RNAs are not fully nested, but crossed in 2D notation. Pseudoknots are abundant in RNA structures in the PDB, and are known to play essential functional roles[36]. However, they possess a challenge to many RNA computational tools, e.g., dynamic programming based prediction of 2D structures. DSSR can characterize pseudoknots of arbitrary complexity in a 3D RNA structure. It also has the capability to remove pseudoknots to produce a nested 2D structure in dbn notation.

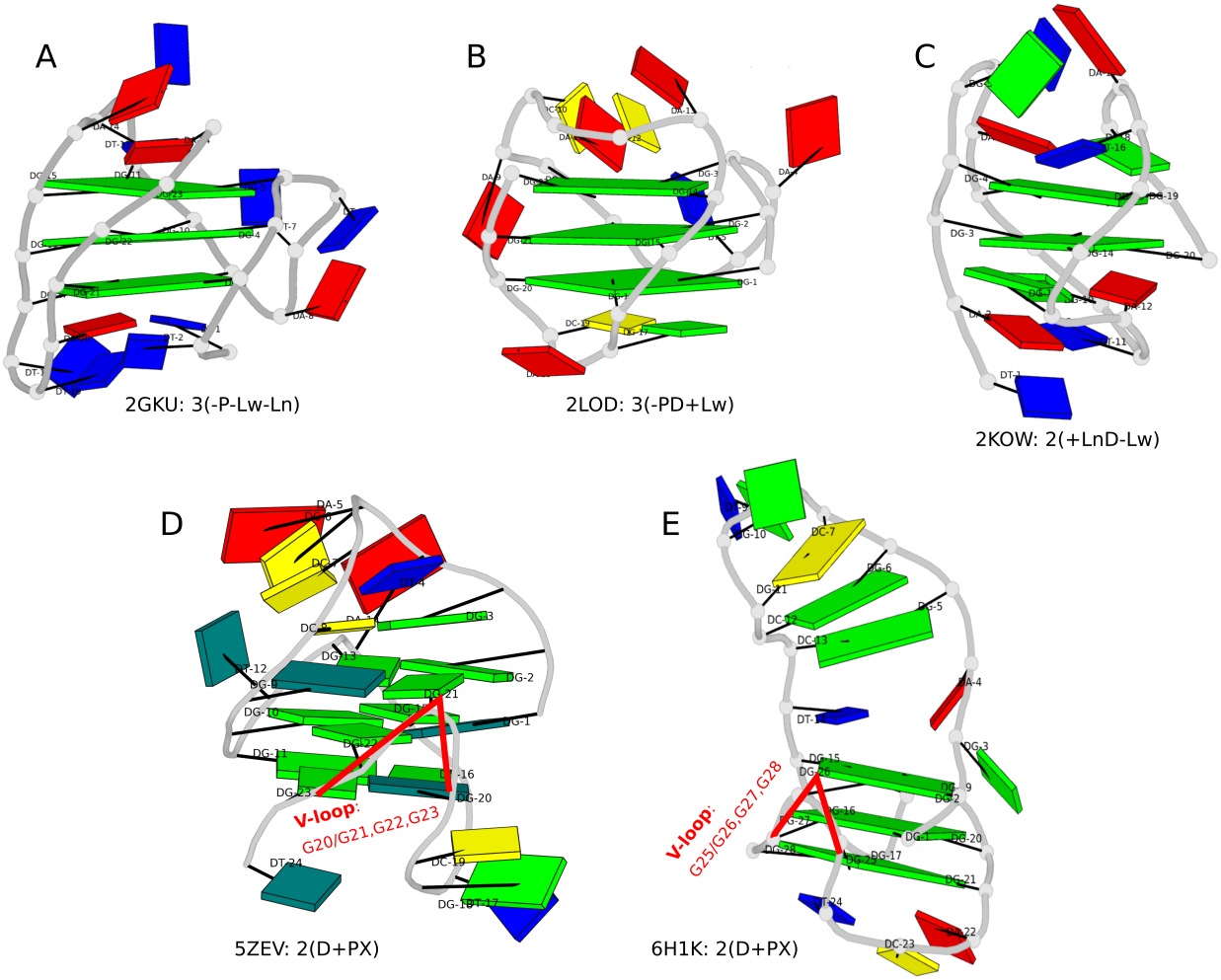

Figure 16: Five G4 structures with revised topological descriptors[35]. It is worth noting that the descriptors for PDB entries 2gku and 2lod as originally reported in Figure 1 of Dvorkin *et al.*[35] are incorrect. Applying DSSR consistently can correct errors from leading experts who proposed the descriptors in the first place. The structural features were automatically derived by DSSR. The images were rendered with PyMOL.

3.6.1 Higher-order pseudoknots

Using PDB entry 1ddy[37] as an example, here is the relevant DSSR output. Note that 1ddy contains four RNA chains (A, C, E, and G), and DSSR handles each correctly. Here WC pairs in the 2nd order pseudoknots are represented as matched curly brackets `{}`. For even higher-order pseudoknots, the WC pairs are represented by matched angle brackets `<>`, and upper-lower case letters (`Aa`, `Bb`, `Cc`, etc.)

```
This structure contains 2-order pseudoknot
   o You may want to run DSSR again with the '--nested' option which removes
     pseudoknots to get a fully nested secondary structure representation.

Secondary structures in dot-bracket notation (dbn) as a whole and per chain
>1ddy nts=140 [whole]
GGAACCGGUGCGCAUAACCACCUCAGUGCGAGCAA&GGAACCGGUGCGCAUAACCACCUCAGUGCGAGCAA&
    ↪ GGAACCGGUGCGCAUAACCACCUCAGUGCGAGCAA&GGAACCGGUGCGCAUAACCACCUCAGUGCGAGCAA
......(((.{[[....[[)))...].].}.]]..&......(((.{[[....[[)))...].].}.]]..&......(((.{[[....[[)
    ↪ )))...].].}.]]..&......(((.{[[....[[)))...].].}.]]..
>1ddy-A #1 nts=35 0.46(2.84) [chain] RNA
GGAACCGGUGCGCAUAACCACCUCAGUGCGAGCAA
......(((.{[[....[[)))...].].}.]]..
>1ddy-C #2 nts=35 0.66(2.88) [chain] RNA
GGAACCGGUGCGCAUAACCACCUCAGUGCGAGCAA
......(((.{[[....[[)))...].].}.]]..
>1ddy-E #3 nts=35 0.72(2.88) [chain] RNA
GGAACCGGUGCGCAUAACCACCUCAGUGCGAGCAA
......(((.{[[....[[)))...].].}.]]..
>1ddy-G #4 nts=35 0.54(2.87) [chain] RNA
GGAACCGGUGCGCAUAACCACCUCAGUGCGAGCAA
......(((.{[[....[[)))...].].}.]]..
```

3.6.2 Pseudoknot removal

A closely related issue is pseudoknot removal, a topic nicely summarized by Smit *et al*[38]. The `--nested` (or abbreviated form `--nest`) option can be used to remove pseudoknots to get a nested 2d structure in dbn. Using PDB entry 1ddy as an example, the relevant DSSR output with option `--nested` is as follows:

```
This structure contains 2-order pseudoknot
   o You have chosen to remove the pseudoknots with the '--nested' option so
     only a fully nested secondary structure representation remains.

Secondary structures in dot-bracket notation (dbn) as a whole and per chain
>1ddy nts=140 [whole]
GGAACCGGUGCGCAUAACCACCUCAGUGCGAGCAA&GGAACCGGUGCGCAUAACCACCUCAGUGCGAGCAA&
    ↪ GGAACCGGUGCGCAUAACCACCUCAGUGCGAGCAA&GGAACCGGUGCGCAUAACCACCUCAGUGCGAGCAA
......(((..........)))............&......(((..........)))............&......(((..........)
    ↪ )))............&......(((..........)))............
>1ddy-A #1 nts=35 0.46(2.84) [chain] RNA
GGAACCGGUGCGCAUAACCACCUCAGUGCGAGCAA
```

```
......(((..........)))............
>1ddy-C #2 nts=35 0.66(2.88) [chain] RNA
GGAACCGGUGCGCAUAACCACCUCAGUGCGAGCAA
......(((..........)))............
>1ddy-E #3 nts=35 0.72(2.88) [chain] RNA
GGAACCGGUGCGCAUAACCACCUCAGUGCGAGCAA
......(((..........)))............
>1ddy-G #4 nts=35 0.54(2.87) [chain] RNA
GGAACCGGUGCGCAUAACCACCUCAGUGCGAGCAA
......(((..........)))............
```

3.7 The `--more` option

The `--more` option triggers additional parameters for several sections, including base pairs, helices, and stems. Since helices/stems share the same format for the added parameters, only an example from stems is shown. In what follows, the excerpted portions are based on PDB entry 1msy with the following DSSR command:

```
x3dna-dssr -i=1msy.pdb --more -o=1msy-more.out
```

3.7.1 Extra characterization of base pairs

The G–U wobble pair formed by `A.G2648` and `A.U2672` (the second bp on Page 13) is used as an example of the additional information provided about bp geometry and H-bonding with the `--more` option (see Figure 17).

```
1   2 A.G2648        A.U2672        G-U Wobble      28-XXVIII cWW  cW-W
2       [-167.8(anti) ~C3'-endo lambda=42.1] [-152.8(anti) ~C3'-endo lambda=68.6]
3       d(C1'-C1')=10.44 d(N1-N9)=8.84 d(C6-C8)=9.70 tor(C1'-N1-N9-C1')=-8.1
4       H-bonds[2]: "O6(carbonyl)-N3(imino)[2.78],N1(imino)-O2(carbonyl)[2.83]"
5       interBase-angle=9  Simple-bpParams: Shear=-2.44 Stretch=-0.01 Buckle=2.7 Propeller
            ↪ =-8.6
6       bp-pars: [-2.37   -0.60   0.11    4.67    -7.75   -2.95]
```

- Line no. 1: specification of the bp, as shown previously on Page 13.
- Line no. 2: the first bracket `[-167.8(anti) C3′-endo lambda=42.1]` corresponds to `A.G2648`, and it contains three items: `-167.8(anti)` is the χ torsion angle formed by `O4′-C1′-N9-C4`, C3′-endo is the sugar pucker (as is the norm for RNA), and λ (lambda) is the angle `N9-C1′-C1′` (`A.U2672`). The second bracket corresponds to `A.U2672`: `[-152.8(anti) C3′-endo lambda=68.6]` with similar meanings for parameters, except that χ is defined by `O4′-C1′-N1-C2`, and λ is the angle `N1-C1′-C1′` (`A.G2648`).

- Line no. 3: lengths of three virtual bonds (`C1′-C1′`, `N1-N9`, `C6-C8`), and the virtual torsion angle (`C1′-N1-N9-C1′`). Note here N1 and N9 are general terms, referring to either N1 of pyrimidines (Y: C/U/T) or N9 of purines (R: A/G) as appropriate. Similar conventions apply for the labeling of C6/C8.
- Line no. 4: detailed H-bonding information (atom names, types, and H-bond distances in square brackets).
- Line no. 5: inter-base-angle (9°), and a set of four 'simple' bp parameters[11] (shear, stretch, buckle and propeller) which are easier to understand than the six rigorous rigid-body parameters (listed below) for non-canonical pairs, especially when opening is ∼180°.
- Line no. 6: the six rigid-body bp parameters in the order of shear, stretch, stagger, buckle, propeller, and opening (see Figure 7).

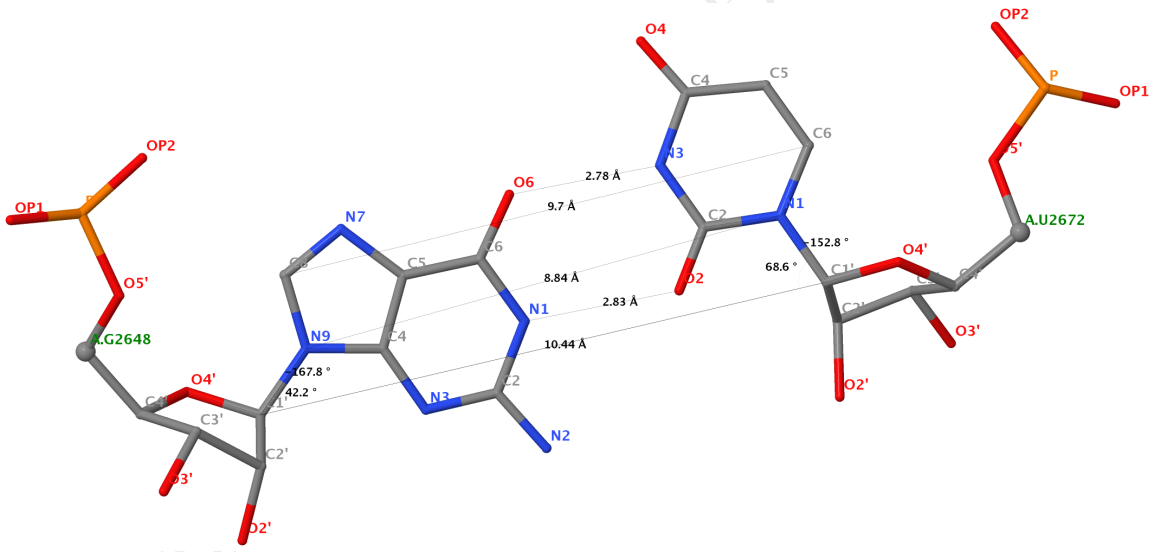

Figure 17: Molecular image of the G–U wobble pair formed by `A.G2648` and `A.U2672` in 1msy, labeled with additional parameters (bond lengths, angles, and torsions). The image was produced with Jmol.

3.7.2 Orientation of helices/stems

The additional output contains information about the best-fitted linear helical axis of a helix/stem, derived using a combination of equivalent C1′ and RN9/YN1 atom pairs along

each strand[39]. The result for the 1msy stem listed on Page 23 is shown below.

```
helical-rise:   2.60(0.18)
helical-radius: 9.12(0.79)
helical-axis:   -0.776    -0.167    -0.608
   point-one:   24.637    21.051    22.830
   point-two:   16.686    19.344    16.602
```

- The `helical-rise` line, with numbers `2.60(0.18)`, represents the average helical rise (`2.60`) between successive nucleotides and its standard deviation (sd, `0.18`) in Å. For a perfectly regular DNA/RNA helix, the sd would be zero. RNA models generated with the DSSR fiber module, for example, are characterized by numbers `2.55(0.00)`. In DSSR, the sd is used to determine if a helix/stem is strongly curved, with a default cutoff of 0.6 Å. If the sd for a helix/stem is over the cutoff (as for the 1msy helix listed on Page 22), a `*` is appended, serving as a reminder that the best-fitted linear helical axis may not be meaningful.

- The `helical-radius` line, with numbers `9.12(0.79)`, gives the average and sd of the perpendicular distances from phosphorus atoms (of both strands) to the helical axis. Typically, the mean radius is around 9.2 Å for double helical DNA or RNA.

- The `helical-axis` line, with three numbers `-0.776 -0.167 -0.608`, provides the normalized helical axis vector (in the original coordinate frame). This vector can be used to calculate DNA bending angles (as in DNA-protein complexes), or to quantify the relative orientation between any two fairly straight helices/stems[10].

- The lines starting with `point-one` and `point-two` designate the end points (in the original coordinate frame) of the helical axis of the helix/stem. The two points can be added to the original PDB coordinates file for visualization of the helical axis or for rendering of helical regions as cylinders[1,10].

3.7.3 Base-pair morphology parameters for helices/stems

The 2nd dinucleotide step consisting of pairs C–G (`A.C2649` with `A.G2671`) and U–A (`A.U2650` with `A.A2670`) in the stems section of 1msy is used here as an example. Six extra lines are enabled by the `--more` option. For the definitions of base and step parameters, see Figure 7.

```
2 A.C2649        A.G2671        C-G WC           19-XIX    cWW  cW-W
     bp1-pars:  [0.09     -0.17    0.02     9.60     -15.93   -2.31]
    step-pars:  [0.79     -1.42    3.25     -0.33    7.26     33.48]
    heli-pars:  [-3.49    -1.39    2.88     12.42    0.57     34.24]
     bp2-pars:  [0.11     -0.11    0.25     4.92     -16.45   6.33]
    C1'-based:                rise=3.25                 twist=33.33
    C1'-based:              h-rise=2.87                h-twist=34.09
3 A.U2650        A.A2670        U-A WC           20-XX     cWW  cW-W
```

- The `bp1-pars` line lists the six bp parameters in the order of shear, stretch, stagger, buckle, propeller, and opening for the C–G pair (`A.C2649` with `A.G2671`).
- The `step-pars` line lists the six step parameters in the order of shift, slide, rise, tilt, roll, and twist for the dinucleotide step between pairs C–G (`A.C2649` with `A.G2671`) and U–A (`A.U2650` with `A.A2670`), calculated based on a middle-step frame[9].
- The `heli-pars` line lists the six helical parameters in the order of x-displacement, y-displacement, helical rise, inclination, tip, and helical twist for the aforementioned dinucleotide step, calculated based on a middle-helical frame[9].
- The `bp2-pars` line lists the six bp parameters in the order of shear, stretch, stagger, buckle, propeller, and opening for the U–A pair (`A.U2650` with `A.A2670`).
- The 1st `C1'-based` line provides rise and twist derived using the two consecutive C1′–C1′ vectors, each defined by a pair in the dinucleotide step. These two parameters are related to the middle-step frame used to calculate the six step parameters listed on the `step-pars` line.
- The 2nd `C1'-based` line provides helical rise and helical twist derived using the two consecutive C1′–C1′ vectors, each defined by a pair in the dinucleotide step. These two parameters are related to the middle-helical frame used to calculate the six helical parameters listed on `heli-pars` line.

3.8 The `--non-pair` option

With the `--non-pair` option, DSSR identifies H-bonding and base-stacking interactions between two nts, excluding those duos that already form a pair. For 1msy, the running command and relevant results are given below.

```
# ~/Luxes/src/academic/DSSR2-src/x3dna-dssr -i=1msy.pdb --non-pair -o=1msy-nonpair.out

List of 30 non-pairing interactions
   1 A.U2647   A.G2648   stacking: 1.0(0.5)--pm(>>,forward) interBase-angle=6 connected min-baseDist=3.26
   2 A.G2648   A.C2649   stacking: 7.3(4.6)--pm(>>,forward) interBase-angle=5 connected min-baseDist=3.30
   3 A.G2648   A.G2673   stacking: 2.0(0.2)--mm(<>,outward) interBase-angle=2 min-baseDist=3.28
   4 A.C2649   A.U2650   stacking: 2.8(1.1)--pm(>>,forward) interBase-angle=9 connected min-baseDist=3.09
   5 A.U2650   A.C2651   stacking: 0.6(0.0)--pm(>>,forward) interBase-angle=7 connected min-baseDist=3.30
   6 A.C2651   A.C2652   stacking: 0.5(0.1)--pm(>>,forward) interBase-angle=12 connected min-baseDist=3.30
   7 A.C2652   A.U2653   stacking: 5.2(2.6)--pm(>>,forward) interBase-angle=13 connected min-baseDist=3.43
   8 A.C2652   A.G2669   stacking: 0.2(0.0)--mm(<>,outward) interBase-angle=7 min-baseDist=3.22
   9 A.U2653   A.A2654   stacking: 3.3(2.0)--pp(><,inward) interBase-angle=13 H-bonds[1]: "OP2-O2'(hydroxyl)[2.62]"
       ↪ connected min-baseDist=3.23
  10 A.A2654   A.U2656   stacking: 3.7(1.1)--mm(<>,outward) interBase-angle=1 H-bonds[1]: "O4'*O4'[3.05]" min-baseDist=3.45
  11 A.G2655   A.G2664   stacking: 4.4(2.2)--pp(><,inward) interBase-angle=10 H-bonds[2]: "O2'(hydroxyl)-O6(carbonyl)
       ↪ [3.09],O2'(hydroxyl)-N1(imino)[3.34]" min-baseDist=3.37
  12 A.G2655   A.A2665   interBase-angle=21 H-bonds[2]: "N1(imino)-OP2[2.77],N2(amino)-O5'[2.89]" min-baseDist=4.79
  13 A.U2656   A.G2664   interBase-angle=7 H-bonds[2]: "OP2-N1(imino)[3.04],OP2-N2(amino)[2.94]" min-baseDist=3.36
  14 A.A2657   A.C2658   stacking: 6.7(2.6)--pm(>>,forward) interBase-angle=4 connected min-baseDist=3.46
  15 A.A2657   A.A2665   stacking: 3.7(3.3)--mm(<>,outward) interBase-angle=11 min-baseDist=3.29
  16 A.C2658   A.G2659   stacking: 0.4(0.1)--pm(>>,forward) interBase-angle=10 connected min-baseDist=3.34
  17 A.G2659   A.A2661   interBase-angle=31 H-bonds[2]: "O2'(hydroxyl)-N7[2.60],O2'(hydroxyl)-N6(amino)[3.26]" min-baseDist
       ↪ =3.97
  18 A.G2659   A.G2663   stacking: 3.9(1.2)--mm(<>,outward) interBase-angle=4 min-baseDist=3.35
  19 A.U2660   A.A2661   stacking: 7.5(4.2)--pm(>>,forward) interBase-angle=17 connected min-baseDist=3.26
  20 A.A2661   A.A2662   stacking: 6.3(4.4)--pm(>>,forward) interBase-angle=19 connected min-baseDist=3.38
  21 A.G2663   A.G2664   stacking: 2.7(0.6)--pm(>>,forward) interBase-angle=8 connected min-baseDist=3.38
  22 A.G2664   A.A2665   interBase-angle=14 H-bonds[1]: "O2'(hydroxyl)-O4'[2.75]" connected min-baseDist=5.83
  23 A.A2665   A.C2666   stacking: 1.6(1.1)--pm(>>,forward) interBase-angle=10 connected min-baseDist=3.18
  24 A.C2666   A.C2667   stacking: 4.3(2.1)--pm(>>,forward) interBase-angle=8 connected min-baseDist=3.35
  25 A.C2667   A.G2668   stacking: 3.1(1.0)--pm(>>,forward) interBase-angle=7 connected min-baseDist=3.38
  26 A.G2668   A.G2669   stacking: 4.3(3.0)--pm(>>,forward) interBase-angle=4 connected min-baseDist=3.28
  27 A.G2669   A.A2670   stacking: 4.3(2.9)--pm(>>,forward) interBase-angle=4 connected min-baseDist=3.29
  28 A.A2670   A.G2671   stacking: 1.5(1.5)--pm(>>,forward) interBase-angle=6 connected min-baseDist=3.24
  29 A.G2671   A.U2672   stacking: 7.4(4.0)--pm(>>,forward) interBase-angle=10 connected min-baseDist=3.22
  30 A.U2672   A.G2673   interBase-angle=11 H-bonds[1]: "O2'(hydroxyl)-O4'[3.37]" connected min-baseDist=3.61
```

Following 3DNA[9], DSSR quantifies base-stacking interactions by the area (in Å^2) of the overlapped polygon defined by the two bases of the interacting nts, where the base atoms are projected onto the mean base plane. In the output file, values in parentheses measure the overlap areas of base ring atoms only, and those outside parentheses include exocyclic atoms.

In DSSR, base-stacking interactions are classified into one of the following four categories: (i) `pm(>>,forward)`, (ii) `mp(<<,backward)`, (iii) `mm(<>,outward)`, and (iv) `pp(><,inward)`. Here `p` and `m` represent the plus and minus faces of the base ring, as defined by the direction of the z-axis of the standard base reference frame[4] (see Figure 1). The symbols (`>>`, `<<`, `<>`, and `><`) follow Major *et al.*, except that `pm(>>)` is called *forward* instead of upward, and `mp(<<)` is named *backward* instead of downward[40].

The term `interBase-angle` represents the inter-base angle; a value close to zero means that the two bases are nearly parallel. The term `connected`, if present, means that the two nucleotides are connected by a covalent phosphodiester linkage. The term `min-baseDist` gives

the minimum distance between base atoms.

The H-bonding information should be self-explanatory, except for a note on convention: when a pair of donor/donor or acceptor/acceptor atoms fulfills the geometry-based H-bond definition in DSSR, the `*` symbol is used instead of `-` to connect the atoms (e.g., entry no. 10: `O4'*O4'[3.05]`).

3.9 The `--json` option

The `--json` option directs DSSR to output results in the standard JSON data exchange format. The single JSON file contains numerous DSSR-derived structural features, including those in the default output, backbone torsions, and H-bonds.

The JSON output makes DSSR readily interoperable with other (bioinformatics) tools. Using tRNA^{Phe} 1ehz as an example, let's go over some use cases with the jq command-line JSON processor.

```
x3dna-dssr -i=1ehz.pdb --json -o=1ehz-dssr.json
jq . 1ehz-dssr.json  # reformatted for pretty output
x3dna-dssr -i=1ehz.pdb --json | jq .  # the above two steps combined
```

With file `1ehz-dssr.json` in hand, one can easily extract DSSR-derived structural features of interest:

```
jq .pairs 1ehz-dssr.json   # list of 34 pairs
jq .multiplets 1ehz-dssr.json  # list of 4 base triplets
jq .hbonds 1ehz-dssr.json  # list of hydrogen bonds
jq .helices 1ehz-dssr.json
jq .stems 1ehz-dssr.json
  # list of nucleotide parameters, including torsion angles and suites
jq .nts 1ehz-dssr.json
  # list of 14 modified nucleotides
jq '.nts[] | select(.is_modified)' 1ehz-dssr.json
  # select nucleotide id, delta torsion, sugar puckering and cluster of suite name
jq '.nts[] | {nt_id, delta, puckering, cluster}' 1ehz-dssr.json
  # same selection as above, but in 'comma-separated-values' (csv) format
jq -r '.nts[] | [.nt_id, .delta, .puckering, .cluster] | @csv' 1ehz-dssr.json
```

Here is the result of running `jq` to select multiplets:

```
# jq .multiplets 1ehz-dssr.json
[
  {
    "index": 1,
    "num_nts": 3,
    "nts_short": "UAA",
    "nts_long": "A.U8,A.A14,A.A21"
  },
```

```
  {
    "index": 2,
    "num_nts": 3,
    "nts_short": "AUA",
    "nts_long": "A.A9,A.U12,A.A23"
  },
  {
    "index": 3,
    "num_nts": 3,
    "nts_short": "gCG",
    "nts_long": "A.2MG10,A.C25,A.G45"
  },
  {
    "index": 4,
    "num_nts": 3,
    "nts_short": "CGg",
    "nts_long": "A.C13,A.G22,A.7MG46"
  }
]
```


3.10 The `--pair-only` option

DSSR provides far more features than a typical user normally need. The `--pair-only` option directs DSSR to output only base-pairing information, the most fundamental aspect in DNA/RNA structural bioinformatics. It can be combined with the `--more` or `--json` option. DSSR runs approximately 10 times faster with the `--pair-only` option than the default.

3.11 The `--nmr` option

The `--nmr` option has been introduced for the analysis of an ensemble of NMR structures, as deposited in the PDB. The input file can be in the `.pdb` format where each model is delineated with MODEL/ENDMDL, or the `.cif` format where each ATOM/HETATM record is associated with a model number.

Using PDB entry 2n2d as an example, two simple usages are as follows:

```
x3dna-dssr -i=2n2d.pdb --nmr -o=2n2d-model.out
x3dna-dssr -i=2n2d.pdb --nmr --json -o=2n2d.json
    jq '.models[].parameters.num_Gtetrads' 2n2d.json
```

The top-level skeleton of the JSON output is shown below. Note that each member of the `models` array contains three items: an auto-incremental `index` (1 to the number of models), the actual `model` number, and the `parameters` object which corresponds to the JSON output if the model is analyzed separately. Normally, `index` and `model` match each other, as is the case for 2n2d. However, it is conceivable that models do not start from one, or the numbers

are not continuous. In such cases, they will no longer have the same value for each entry.

```
{
  "input_file": "2n2d.pdb",
  "num_models": 10,
  "models": [
    {
      "index": 1,
      "model": 1,
      "parameters": { ... }
    },
    ...
    {
      "index": 10,
      "model": 10,
      "parameters": { ... }
    }
  ],
  "start_at": "Thu Aug 20 00:06:03 2020",
  "finish_at": "Thu Aug 20 00:06:04 2020",
  "time_used": "00:00:00:01"
}
```

The `--json` option makes it easy to parse the output of multiple models pragmatically. In addition to NMR structures, trajectories from molecular dynamics (MD) simulations can also be processed. As noted above, DSSR takes only the standard `.pdb` or `.cif` format for input. Thus, proprietary binary formats for trajectories from popular MD packages need to be converted to a standard format. The combination of `--nmr` and `--json` renders DSSR easily accessible to the MD community. The Pro version of DSSR has a far more efficient engine than the Basic one for pragmatic analyses of MD trajectories.

3.12 The `--get-hbond` option

H-bonding interactions are crucial for defining RNA secondary and tertiary structures. DSSR contains a geometrically based algorithm for identifying H-bonds in nucleic-acid or protein structures specified in `.pdb` or `.cif` format. Over the years, the method has been continuously refined, and it has served its purpose quite well. This functionality is also directly available through the `--get-hbond` option. By default, the output only includes H-bonds involving nucleotides.

```
x3dna-dssr -i=1msy.pdb --get-hbond -o=1msy-hbonds.txt
```

Running the above command, the output for 1msy is as listed below. The 1st line is the header ("`# H-bonds in '1msy.pdb' identified by DSSR` ..."). The 2nd line provides the

total number of H-bonds (40) identified in the structure. Afterwards, each line consists of eight space-delimited columns used to characterize a specific H-bond. Using the first H-bond as an example, the meaning of each of the eight columns is detailed below:

1. The serial number (15), as denoted in the .pdb or .cif file, of the 1st atom of the H-bond.
2. The serial number (578) of the 2nd atom of the H-bond.
3. The H-bond index (#1), a serial number from 1 to the total number of H-bonds.
4. A one-letter symbol showing the atom-pair type (p) of the H-bond. It is p for a donor-acceptor atom pair; o for a donor/acceptor (such as the 2′-hydroxyl oxygen) with any other atom; x for a donor-donor or acceptor-acceptor pair (as in #17); ? if the donor/acceptor status of any H-bond atom is unknown.
5. Distance between donor/acceptor atoms in Å (2.768).
6. Elemental symbols of the two atoms involved in the H-bond (O:N).
7. Identifier of the 1st H-bonded atom (O4@A.U2647).
8. Identifier of the 2nd H-bonded atom (N1@A.G2673).

```
# H-bonds in '1msy.pdb' identified by DSSR
40
   15    578   #1      p     2.768 O:N O4@A.U2647 N1@A.G2673
   35    555   #2      p     2.776 O:N O6@A.G2648 N3@A.U2672
   36    554   #3      p     2.826 N:O N1@A.G2648 O2@A.U2672
   55    537   #4      p     2.965 O:N O2@A.C2649 N2@A.G2671
   56    535   #5      p     2.836 N:N N3@A.C2649 N1@A.G2671
   58    534   #6      p     2.769 N:O N4@A.C2649 O6@A.G2671
   76    513   #7      p     2.806 N:N N3@A.U2650 N1@A.A2670
   78    512   #8      p     3.129 O:N O4@A.U2650 N6@A.A2670
   95    492   #9      p     2.703 O:N O2@A.C2651 N2@A.G2669
   96    490   #10     p     2.853 N:N N3@A.C2651 N1@A.G2669
   98    489   #11     p     2.987 N:O N4@A.C2651 O6@A.G2669
  115    466   #12     p     2.817 O:N O2@A.C2652 N2@A.G2668
  116    464   #13     p     2.907 N:N N3@A.C2652 N1@A.G2668
  118    463   #14     p     2.897 N:O N4@A.C2652 O6@A.G2668
  123    151   #15     o     2.622 O:O OP2@A.U2653 O2'@A.A2654
  135    443   #16     p     2.898 O:N O2@A.U2653 N4@A.C2667
  147    192   #17     x     3.054 O:O O4'@A.A2654 O4'@A.U2656
  158    408   #18     p     2.960 N:O N6@A.A2654 OP2@A.C2666
  173    188   #19     o     2.923 O:O O2'@A.G2655 OP2@A.U2656
  173    378   #20     o     3.093 O:O O2'@A.G2655 O6@A.G2664
  173    379   #21     o     3.343 O:N O2'@A.G2655 N1@A.G2664
  181    386   #22     p     2.768 N:O N1@A.G2655 OP2@A.A2665
```

```
  183   203  #23    p    2.754 N:O N2@A.G2655 O4@A.U2656
  183   387  #24    p    2.887 N:O N2@A.G2655 O5'@A.A2665
  188   379  #25    p    3.044 O:N OP2@A.U2656 N1@A.G2664
  188   381  #26    p    2.944 O:N OP2@A.U2656 N2@A.G2664
  200   401  #27    p    3.122 O:N O2@A.U2656 N6@A.A2665
  201   398  #28    p    2.759 N:N N3@A.U2656 N7@A.A2665
  220   381  #29    p    3.035 N:N N7@A.A2657 N2@A.G2664
  223   371  #30    o    2.963 N:O N6@A.A2657 O2'@A.G2664
  223   382  #31    p    3.039 N:N N6@A.A2657 N3@A.G2664
  242   358  #32    p    2.821 O:N O2@A.C2658 N2@A.G2663
  243   356  #33    p    2.890 N:N N3@A.C2658 N1@A.G2663
  245   355  #34    p    2.887 N:O N4@A.C2658 O6@A.G2663
  258   305  #35    o    2.604 O:N O2'@A.G2659 N7@A.A2661
  258   308  #36    o    3.264 O:N O2'@A.G2659 N6@A.A2661
  268   315  #37    p    2.973 N:O N2@A.G2659 OP2@A.A2662
  268   327  #38    p    2.864 N:N N2@A.G2659 N7@A.A2662
  371   390  #39    o    2.751 O:O O2'@A.G2664 O4'@A.A2665
  550   566  #40    o    3.372 O:O O2'@A.U2672 O4'@A.G2673
```

In its default settings (`--get-hbond`, same as `--get-hbond=nuc`), DSSR detects 118 H-bonds for 1ehz and 5,809 H-bonds for 1jj2 among nucleotides, respectively. By including `protein` (or `amino`) in the option, as in `--get-hbond=nuc-protein`, the program also outputs H-bonds in proteins or at the RNA/protein interfaces. For 1jj2, DSSR now detects a total of 10,583 H-bonds.

Overall, the H-bonding identification method in DSSR is robust and efficient, extensively tested with nucleic-acid-containing structures in the PDB. While there exist dedicated tools for finding H-bonds, such as HBPLUS or HBexplore, DSSR may well server as a pragmatic tool for most applications.

3.13 The `--idstr` option

By default, the identifier for nts in DSSR looks like `A.U2647`. DSSR offers two additional variations, `--idstr=long` and `--idstr=short`, to serve different purposes. Shown below are the listings for a 1msy pair, with three `--idstr` variations.

```
# without the --idstr option (default)
   1 A.U2647        A.G2673        U-G --          --        cWW  cW-W
# with the --idstr=long option
   1 ..A.U.2647.    ..A.G.2673.    U-G --          --        cWW  cW-W
# with the --idstr=short option
   1 U2647          G2673          U-G --          --        cWW  cW-W
```

The long id string consists of six components, which are put in strict order, as given below. A complete example—with model number 1, no segid, chain id C, residue name A (for adenosine), sequence number 24, and insertion code L—is `1..C.A.24.L`. The corresponding

short form is A24.

```
model-number.segid.chain-id.residue-name.residue-number.insertion-code
```

3.14 The --symmetry option

By default, DSSR only analyzes the first structure (model) in a given .pdb for .cif file. For x-ray crystal structures, the asymmetric unit may contain only a faction of the biological unit. As an example, the asymmetric unit of PDB entry 4ms9 is single-stranded (4ms9.pdb), while the biological unit is a double helix (4ms9.pdb1).

Running DSSR on 4ms9.pdb, or 4ms9.pdb1 with default settings, finds no base pairs. In such cases, one needs to use the --symmetry (short form --symm) option as shown below for the desired result:

```
x3dna-dssr -i=4ms9.pdb1 --symm
```

DSSR just reads ATOM/HETATM records, as provided in the coordinates file. It does not perform auto-expansion of an asymmetric unit into biological unit based on crystallographic symmetric information that may exist in the .pdb or .cif file. Users must supply the biological unit file (4ms9.pdb1) and the specify the --symm option for the desired result.

3.15 The --prefix option

By default, DSSR auxiliary output files are prefixed with dssr, as in dssr-pairs.pdb. The fixed generic names are overwritten on repeated DSSR runs in a directory. With the --prefix=text option, the auxiliary output files will be prefixed by text. For example, with the following command, the auxiliary output files will be named 1ehz-pairs.pdb, etc.

```
x3dna-dssr -i=1ehz.pdb -o=1ehz.out --prefix=1ehz
```

4 Visualization features

DSSR can be easily incorporated into other structural bioinformatics pipelines. Over the years, I have been fortunate to collaborate with Robert Hanson and Thomas Holder to

connect DSSR to Jmol and PyMOL, respectively. These integrations led to two peer-reviewed articles, "DSSR-enhanced visualization of nucleic acid structures in Jmol"[2] and "DSSR-enabled innovative schematics of 3D nucleic acid structures with PyMOL"[3], both published in *Nucleic Acids Research*. They also exemplify the critical roles that a domain-specific analysis engine may play in general-purpose molecular visualization tools.

The DSSR-Jmol integration excels in its SQL-like, flexible searching capability of structural features. The DSSR-PyMOL integration, on the other hand, stands out for the appealing cartoon-block schematics it brings.

4.1 DSSR-Jmol integration

The "DSSR-Jmol integration" section on the 3DNA Forum contains scripts and data files for reproducing reported results, including the graphical abstract and the cover image (Figure 18).

Overall, the DSSR-Jmol integration makes salient features of DSSR readily accessible via Jmol/JSmol, as demonstrated at the website http://jmol.x3dna.org. This work fills a gap in RNA structural bioinformatics. It enables deep analyses and SQL-like queries of RNA structural characteristics, interactively.

4.2 DSSR-PyMOL integration

The DSSR-PyMOL integration brings unprecedented visual clarity to 3D nucleic acid structures, especially for G-quadruplexes (see Figures 15 and 16). These features can be accessed via four interfaces: the command-line interface, the DSSR plugin for PyMOL, the web application, and the web application programming interface. The easiest way to get started and quickly benefit from this work is via the web application at http://skmatic.x3dna.org. Please refer to the paper[3] and the corresponding supplemental PDF for details.

The website http://skmatic.x3dna.org has been recommended in Faculty Opinions as "simple and effective", and classified as "Good for Teaching".

5 Modeling capabilities

DSSR Pro comes with three modeling modules: (i) `mutate` for *in silico* (base) mutations, (ii) `fiber` for generating regular helical models, and (iii) `rebuild` for creating customized

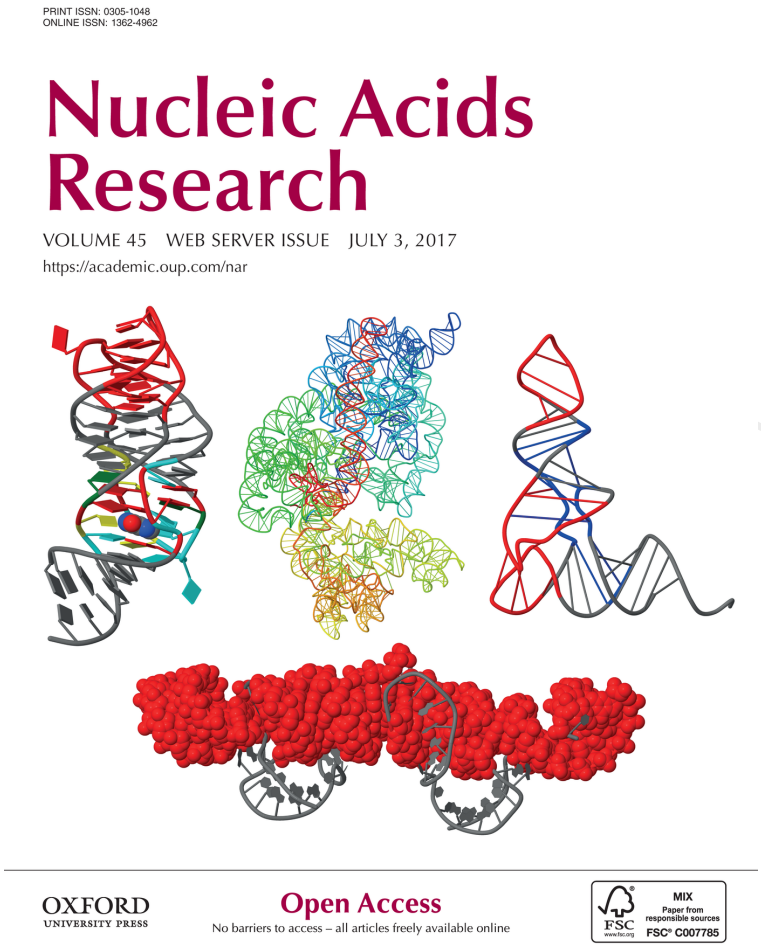

Figure 18: 3D interactive visualization of selected RNA structural features enabled by the DSSR-Jmol integration (http://jmol.x3dna.org). Clockwise from upper left: Structure of the xpt-pbuX guanine riboswitch in complex with hypoxanthine (PDB entry 4fe5) in 'base blocks' representation. The three-way junction loop encompassing the metabolite (in space-filling representation) is color-coded by base identity: A, red; C, yellow; G, green; U, cyan. The loop-loop interaction at the top is highlighted in red. Structure of the *T. thermophilus* 30S ribosomal subunit in complex with antibiotics (PDB entry 1fjg) in step diagram. The 16S rRNA is color-coded in spectrum with the 5′-end in blue and the 3′-end in red (upper middle). Structure of the classic L-shaped yeast $tRNA^{Phe}$ (PDB entry 1ehz) in step diagram, with the three hairpin loops highlighted in red and the four-way junction loop in blue (upper right corner). Structure of the Pistol self-cleaving ribozyme (PDB entry 5ktj), showcasing (in red) the horizontal helix in space-filling representation. The helix is composed of six short stems stabilized via coaxial stacking interactions (bottom).

structures. They replace the 3DNA `mutate_bases`, `fiber`, and `rebuild` programs, with significantly enhanced features and dramatically improved usability.

These features are documented in the DSSR Pro User Manual (licensed to paid users only).

6 Frequently asked questions

6.1 What does DSSR stand for?

DSSR stands for **D**issecting the **S**patial **S**tructure of **R**NA. It could also mean **D**efining the **S**econdary **S**tructure of **R**NA. Note that DSSR has far more to offer than just defines RNA 2D structures as DSSP does for proteins. The acronym may have other interpretations.

6.2 How does DSSR compare with other tools?

Dozens of software programs and online resources are currently in use for nucleic acid structural bioinformatics. It is fair to say that each has its unique features and no two tools are identical. Comparative studies as seen in the literature are useful for general understanding of a topic. Without going into technical details, however, such comparisons are mostly superficial and seldomly convincing. See my early paper on "Resolving the discrepancies among nucleic acid conformational analyses" [41].

DSSR is an integrated and automated computational tool designed from the bottom up to streamline RNA structural bioinformatics. It possesses a combined set of functionalities well beyond the scope of any other software tools in the field. As a simple example, users are encouraged to compare DSSR with any other tools on the classic yeast $tRNA^{Phe}$ (1ehz, see Section 3.3). Pay close attention to the fact that 1ehz contains 14 modified nucleotides. Among other features, yeast $tRNA^{Phe}$ has four base triplets, two helices corresponding to the L-shaped tertiary structure, four stems matching the cloverleaf 2D structure, three hairpin loops, and a [2,1,5,0] four-way junction loop.

6.3 How is DSSR related to 3DNA?

From a historical perspective, DSSR is built upon the 3DNA suite of software programs for the analysis, rebuilding, and visualization of 3D nucleic acid structures[9–11]. 3DNA takes advantage of standard base reference frame[4], enabled by our contributions on resolving the

discrepancies among nucleic acid conformational analyses[41,42]. 3DNA had also benefitted greatly from the SCHNAaP and SCHNArP pair of programs for rigorous analysis and reversible rebuilding of double-helical nucleic acid structures[39,43]. Specifically, the algorithms that underpinned SCHNAaP/SCHNArP laid the foundation of `analyze/rebuild`, two core components of the 3DNA suite.

Just as 3DNA has replaced SCHNAaP/SCHNArP in functionality and real-world applications, DSSR has superseded 3DNA. Key 3DNA features for analysis, visualization, modeling, and utilities have been integrated into DSSR, with vastly enhanced functionality and significantly improved usability. Notably, the mutate/fiber/rebuild modules in DSSR completely supersedes the `mutate_bases`, `fiber`, and `rebuild` programs distributed with 3DNA v2.4. In short, 3DNA is becoming the past; DSSR is the future.

6.4 What are the differences between DSSR Basic and DSSR Pro?

DSSR Pro contains more features than documented here for the Basic version. DSSR Pro has advanced modeling modules that are missing in the Basic version. DSSR Pro comes with a comprensive user manual that is currently over 230 pages. DSSR Pro can be taken as X3DNA since it completely supersedes 3DNA v2.4. If you find a feature missing in the Basic version, it is likely to be available in DSSR Pro. Moreover, user support, software maintenance and further development are devoted to DSSR Pro.

7 Acknowledgements

The development of DSSR has been made possible by the NIH grant R01GM096889. I'd like to thank Drs. Wilma Olson and Harmen Bussemaker for helpful discussions. I appreciate the user community for providing feedback.

References

1. Lu, X.-J., Bussemaker, H. J., and Olson, W. K. (2015) DSSR: An integrated software tool for dissecting the spatial structure of RNA. *Nucleic Acids Res.,* **43**(21), e142.

2. Hanson, R. M. and Lu, X.-J. (2017) DSSR-enhanced visualization of nucleic acid structures in Jmol. *Nucleic Acids Res.,* **45**(W1), W528–W533.

3. Lu, X.-J. (2020) DSSR-enabled innovative schematics of 3D nucleic acid structures with PyMOL. *Nucleic Acids Res.,* **48**(13), e74.

4. Olson, W. K., Bansal, M., Burley, S. K., Dickerson, R. E., Gerstein, M., Harvey, S. C., Heinemann, U., Lu, X.-J., Neidle, S., Shakked, Z., Sklenar, H., Suzuki, M., Tung, C.-S., Westhof, E., Wolberger, C., and Berman, H. M. (2001) A standard reference frame for the description of nucleic acid base-pair geometry. *J. Mol. Biol.,* **313**(1), 229–237.

5. Saenger, W. (1984) Principles of nucleic acid structure, Springer advanced texts in chemistrySpringer-Verlag, New York first edition.

6. Leontis, N. B. and Westhof, E. (2001) Geometric nomenclature and classification of RNA base pairs. *RNA,* **7**(4), 499–512.

7. Darty, K., Denise, A., and Ponty, Y. (2009) VARNA: Interactive drawing and editing of the RNA secondary structure. *Bioinformatics,* **25**(15), 1974–5.

8. Richardson, J. S., Schneider, B., Murray, L. W., Kapral, G. J., Immormino, R. M., Headd, J. J., Richardson, D. C., Ham, D., Hershkovits, E., Williams, L. D., Keating, K. S., Pyle, A. M., Micallef, D., Westbrook, J., and Berman, H. M. (2008) RNA backbone: consensus all-angle conformers and modular string nomenclature. *RNA,* **14**(3), 465–81.

9. Lu, X.-J. and Olson, W. K. (2003) 3DNA: A software package for the analysis, rebuilding and visualization of three-dimensional nucleic acid structures. *Nucleic Acids Res.,* **31**(17), 5108–5121.

10. Lu, X.-J. and Olson, W. K. (2008) 3DNA: A versatile, integrated software system for the analysis, rebuilding and visualization of three-dimensional nucleic-acid structures. *Nat. Protoc.,* **3**(7), 1213–1227.

11. Li, S., Olson, W. K., and Lu, X.-J. (2019) Web 3DNA 2.0 for the analysis, visualization, and modeling of 3D nucleic acid structures. *Nucleic Acids Res.,* **47**(W1), W26–W34.

12. Correll, C. C., Beneken, J., Plantinga, M. J., Lubbers, M., and Chan, Y.-L. (2003) The common and the distinctive features of the bulged-G motif based on a 1.04 A resolution RNA structure. *Nucleic Acids Res.,* **31**(23), 6806–6818.

13. Lu, X. J., Olson, W. K., and Bussemaker, H. J. (2010) The RNA backbone plays a crucial role in mediating the intrinsic stability of the GpU dinucleotide platform and the GpUpA/GpA miniduplex. *Nucleic Acids Res.,* **38**(14), 4868–76.

14. Gesteland, R. F., Cech, T., and Atkins, J. F. (1999) The RNA world: the nature of modern RNA suggests a prebiotic RNA world, Number 37 in Cold Spring Harbor monograph seriesCold Spring Harbor Laboratory Press, Cold Spring Harbor, NY second edition.

15. Lemieux, S. and Major, F. (2002) RNA canonical and non-canonical base pairing types: a recognition method and complete repertoire. *Nucleic Acids Res.,* **30**(19), 4250–63.

16. Nissen, P., Ippolito, J. A., Ban, N., Moore, P. B., and Steitz, T. A. (2001) RNA tertiary interactions in the large ribosomal subunit: the A-minor motif. *Proc. Natl. Acad. Sci.,* **98**(9), 4899–903.

17. Olson, W. K., Li, S., Kaukonen, T., Colasanti, A. V., Xin, Y., and Lu, X.-J. (2019) Effects of noncanonical base pairing on RNA folding: structural context and spatial arrangements of G·A pairs. *Biochemistry,* **58**(20), 2474–2487.

18. Quigley, G. and Rich, A. (1976) Structural domains of transfer RNA molecules. *Science,* **194**(4267), 796–806.

19. Drew, H. R., Wing, R. M., Takano, T., Broka, C., Tanaka, S., Itakura, K., and Dickerson, R. E. (1981) Structure of a B-DNA dodecamer: conformation and dynamics. *Proc Natl Acad Sci U A,* **78**(4), 2179–83.

20. Lu, X. J., Shakked, Z., and Olson, W. K. (2000) A-form conformational motifs in ligand-bound DNA structures. *J. Mol. Biol.,* **300**(4), 819–40.

21. Chen, V. B., Arendall, W. B., Headd, J. J., Keedy, D. A., Immormino, R. M., Kapral, G. J., Murray, L. W., Richardson, J. S., and Richardson, D. C. (2010) MolProbity: all-atom structure validation for macromolecular crystallography. *Acta Crystallogr. D Biol. Crystallogr.,* **66**(1), 12–21.

22. Olson, W. K. (1980) Configurational statistics of polynucleotide chains. An updated virtual bond model to treat effects of base stacking. *Macromolecules,* **13**(3), 721–728.

23. Keating, K. S., Humphris, E. L., and Pyle, A. M. (2011) A new way to see RNA. *Q. Rev. Biophys.,* **44**(4), 433–66.

24. Altona, C. and Sundaralingam, M. (1972) Conformational analysis of the sugar ring in nucleosides and nucleotides. A new description using the concept of pseudorotation. *J Am Chem Soc,* **94**(23), 8205–12.

25. Zhang, H., Endrizzi, J. A., Shu, Y., Haque, F., Sauter, C., Shlyakhtenko, L. S., Lyubchenko, Y., Guo, P., and Chi, Y.-I. (2013) Crystal structure of 3WJ core revealing divalent ion-promoted thermostability and assembly of the phi29 hexameric motor pRNA. *RNA,* **19**(9), 1226–1237.

26. Nguyen, L. A., Wang, J., and Steitz, T. A. (2017) Crystal structure of Pistol, a class of self-cleaving ribozyme. *Proc Natl Acad Sci USA,* **114**(5), 1021–1026.

27. Cate, J. H., Gooding, A. R., Podell, E., Zhou, K., Golden, B. L., Kundrot, C. E., Cech, T. R., and Doudna, J. A. (1996) Crystal structure of a group I ribozyme domain: principles of RNA packing. *Science,* **273**(5282), 1678–85.

28. Klein, D. J., Schmeing, T. M., Moore, P. B., and Steitz, T. A. (2001) The kink-turn: a new RNA secondary structure motif. *EMBO J.,* **20**(15), 4214–21.

29. Lilley, D. M. (2012) The structure and folding of kink turns in RNA. *WIREs RNA,* **3**(6), 797–805.

30. Wang, J., Daldrop, P., Huang, L., and Lilley, D. M. J. (2014) The k-junction motif in RNA structure. *Nucleic Acids Res.,* **42**(8), 5322–5331.

31. Burge, S., Parkinson, G. N., Hazel, P., Todd, A. K., and Neidle, S. (2006) Quadruplex DNA: Sequence, topology and structure. *Nucleic Acids Res.,* **34**(19), 5402–5415.

32. Rhodes, D. and Lipps, H. J. (2015) G-quadruplexes and their regulatory roles in biology. *Nucleic Acids Res.,* **43**(18), 8627–8637.

33. Lightfoot, H. L., Hagen, T., Tatum, N. J., and Hall, J. (2019) The diverse structural landscape of quadruplexes. *FEBS Lett.,* **593**(16), 2083–2102.

34. Meier, M., Moya-Torres, A., Krahn, N. J., McDougall, M. D., Orriss, G. L., McRae, E. K. S., Booy, E. P., McEleney, K., Patel, T. R., McKenna, S. A., and Stetefeld, J. (2018) Structure and hydrodynamics of a DNA G-quadruplex with a cytosine bulge. *Nucleic Acids Res.,* **46**(10), 5319–5331.

35. Dvorkin, S. A., Karsisiotis, A. I., and Webba da Silva, M. (2018) Encoding canonical DNA quadruplex structure. *Sci. Adv.,* **4**(8), eaat3007.

36. Theimer, C. A., Blois, C. A., and Feigon, J. (2005) Structure of the human telomerase RNA pseudoknot reveals conserved tertiary interactions essential for function. *Mol. Cell,* **17**(5), 671–682.

37. Sussman, D., Nix, J. C., and Wilson, C. (2000) The structural basis for molecular recognition by the vitamin B 12 RNA aptamer. *Nat. Struct. Biol.,* **7**(1), 53–57.

38. Smit, S., Rother, K., Heringa, J., and Knight, R. (2008) From knotted to nested RNA structures: A variety of computational methods for pseudoknot removal. *RNA,* **14**(3), 410–416.

39. Lu, X.-J., El Hassan, M., and Hunter, C. (1997) Structure and conformation of helical nucleic acids: Analysis program (SCHNAaP). *J. Mol. Biol.,* **273**(3), 668–680.

40. Parisien, M., Cruz, J. A., Westhof, E., and Major, F. (2009) New metrics for comparing and assessing discrepancies between RNA 3D structures and models. *RNA,* **15**(10), 1875–1885.

41. Lu, X. J. and Olson, W. K. (1999) Resolving the discrepancies among nucleic acid conformational analyses. *J. Mol. Biol.,* **285**(4), 1563–75.

42. Lu, X.-J., Babcock, M. S., and Olson, W. K. (1999) Overview of Nucleic Acid Analysis Programs. *J. Biomol. Struct. Dyn.,* **16**(4), 833–843.

43. Lu, X.-J., El Hassan, M., and Hunter, C. (1997) Structure and conformation of helical nucleic acids: Rebuilding program (SCHNArP). *J. Mol. Biol.,* **273**(3), 681–691.